Interaptin, an Actin-binding Protein of the α-Actinin Superfamily in *Dictyostelium discoideum*, Is Developmentally and cAMP-regulated and Associates with Intracellular Membrane Compartments

Francisco Rivero,*‡ Adam Kuspa,§ Regine Brokamp,* Monika Matzner,* and Angelika A. Noegel*‡

*Max-Planck-Institut für Biochemie, 82152 Martinsried, Germany; ‡Institut für Biochemie I, Medizinische Fakultät, Universität zu Köln, 50931 Köln, Germany; and §Department of Biochemistry, Baylor College of Medicine, Houston, Texas 77030

Abstract. In a search for novel members of the α-actinin superfamily, a *Dictyostelium discoideum* genomic library in yeast artificial chromosomes (YAC) was screened under low stringency conditions using the acting-binding domain of the gelation factor as probe. A new locus was identified and 8.6 kb of genomic DNA were sequenced that encompassed the whole *abpD* gene. The DNA sequence predicts a protein, interaptin, with a calculated molecular mass of 204,300 D that is constituted by an actin-binding domain, a central coiled-coil rod domain and a membrane-associated domain. In Northern blot analyses a cAMP-stimulated transcript of 5.8 kb is expressed at the stage when cell differentiation occurs. Monoclonal antibodies raised against bacterially expressed interaptin polypeptides recognized a 200-kD developmentally and cAMP-regulated protein and a 160-kD constitutively expressed protein in Western blots. In multicellular structures, interaptin appears to be enriched in anterior-like cells which sort to the upper and lower cups during culmination. The protein is located at the nuclear envelope and ER. In mutants deficient in interaptin development is delayed, but the morphology of the mature fruiting bodies appears normal. When starved in suspension *abpD*$^-$ cells form EDTA-stable aggregates, which, in contrast to wild type, dissociate. Based on its domains and location, interaptin constitutes a potential link between intracellular membrane compartments and the actin cytoskeleton.

Key words: actin cytoskeleton • *Dictyostelium* • green fluorescent protein • development • cyclic AMP

THE cytoskeletal proteins that share the actin-binding domain (ABD)[1] of α-actinin constitute an expanding superfamily. In *Dictyostelium discoideum*, this superfamily comprises α-actinin (Noegel et al., 1987), gelation factor (ABP-120; Noegel et al., 1989), cortexillins I and II (Faix et al., 1996), fimbrin (Prassler et al., 1997), a filamin-like protein (Hock and Condeelis, 1987), and a spectrin-like protein (Bennett and Condeelis, 1988). Additional members have been described in mammalian cells, like dystrophin (Hammonds, 1987), plectin (Liu et al., 1996), and dystonin (Brown et al., 1995). All these proteins are characterized by a modular organization (Matsudaira, 1991), and share a conserved 250–amino acid F-actin–binding domain usually located at the NH_2-terminal end. The three-dimensional structure of an ABD has been resolved recently, and was shown to consist of two α-helical subdomains connected by a long central α-helix (Goldsmith et al., 1997). Members of this superfamily differ in their rod and regulatory domains, which are responsible for oligomerization, calcium regulation, membrane association, or interaction with other proteins. For example, fimbrin, α-actinin, spectrin, and dystrophin possess calmodulin-like calcium binding domains that allow for calcium regulation of their actin-binding activity. Thus, modular organization allows for an ample degree of local and functional specialization of each member of the α-actinin superfamily.

Members of the α-actinin superfamily are also involved in the pathogenesis of disease. Spectrin is required for the stability of many membrane skeletons and defects in

Address all correspondence to Angelika A. Noegel, Institut für Biochemie I, Medizinische Fakultät, Universität zu Köln, Joseph-Stelzmann-Str. 52, 50931 Köln, Germany. Tel.: 49 221 478 6980. Fax: 49 221 478 6979. E-mail: noegel@uni-koeln.de

1. *Abbreviations used in this paper*: ABD, actin-binding domain; ALC, anterior-like cells; BPAG-1, pemphigoid antigen 1; Bsr, blasticidin; DAPI, 4′,6-diamidino-2-phenylindole; GSE, G-rich sequence elements; MAD, membrane-associated domain; PDI, protein disulfide isomerase; PIP2, phosphatidylinositol (4,5) bisphosphate; PVDF, polyvinylidene difluoride; YAC, yeast artificial chromosomes.

© The Rockefeller University Press, 0021-9525/98/08/735/16 $2.00

β-spectrin result in hemolytic anemia (Gallagher and Forget, 1993). Dystrophin associates with a membrane glycoprotein complex through its COOH-terminal domain, thus anchoring the subsarcolemmal actin cytoskeleton to the extracellular matrix in skeletal muscle (Campbell, 1995). Mutations in the gene that encodes dystrophin are responsible for the Duchenne and Becker muscular dystrophies, characterized by skeletal muscle degeneration (Hoffman et al., 1987). Plectin and dystonin possess a COOH-terminal domain responsible for binding to intermediate filaments. These two proteins localize to hemidesmosomes and play an important role connecting actin microfilaments to intermediate filaments. In humans, mutations in the plectin gene are responsible for epidermolysis bullosa with muscular dystrophy. In mice, mutations in the dystonin gene lead to a neurodegenerative disease accompanied by epidermolysis bullosa (reviewed in Fuchs and Cleveland, 1998).

Dictyostelium has emerged as a useful model for studying the actin cytoskeleton. *Dictyostelium* amebae possess a cytoskeleton comparable in its complexity to that of polymorphonuclear leukocytes (Noegel et al., 1997). Furthermore, the ease with which a variety of genetic approaches can be used to generate mutants has made possible the creation of cells with mutations in one or two actin cross-linking proteins, with the result that in most cases single mutants are either normal or display only moderate defects, whereas more profound defects are apparent in double mutants lacking certain combinations of actin cross-linkers (Witke et al., 1992; Faix et al., 1996; Rivero et al., 1996*a*,*b*). In the mouse, an analogous example has been recently reported. Mice lacking either dystrophin or utrophin (the autosomal homologue of dystrophin), display only mild phenotypes, whereas double knockout mutants show severe progressive muscular dystrophy (Grady et al., 1997). This has led to the view that the actin cross-linkers constitute a functional network in which distinct components preferentially perform distinct functions and additionally overlap with each other in a cooperative manner (Rivero et al., 1996*b*).

To have a definitive picture of the events that take place during rearrangement of the actin cytoskeleton we must identify all the components involved. Therefore, we searched for novel members of the α-actinin superfamily in *Dictyostelium*. To this end, a genomic library in yeast artificial chromosomes (YAC; Kuspa et al., 1992) was screened under low stringency conditions using a probe that encodes the ABD of the gelation factor. The new locus identified, *abpD*, encodes a protein of 204.3 kD constituted by an NH_2-terminal ABD, a central coiled-coil rod domain, and a COOH-terminal membrane-associated domain (MAD). Accumulation of *abpD* mRNA is developmentally regulated and stimulated by cAMP, which is unusual for a cytoskeletal protein gene. Immunofluorescence and biochemical studies indicate an association with membranes of intracellular compartments like the nuclear envelope and the ER. Homologous recombination was used to inactivate the *abpD* gene. When starved in suspension *abpD*$^-$ cells are able to build multicellular aggregates, which later dissociate into single cells probably due to a defect in the processing and/or secretion of late adhesion molecules. We have named this protein interaptin (Latin interaptus, bound to each other), since it may constitute a link between intracellular membrane compartments and the actin cytoskeleton, and may thus be involved in the trafficking of secretory vesicles among different intracellular compartments.

Materials and Methods

Cloning of abpD

A cDNA fragment of the gelation factor that corresponds to the ABD (amino acids 1–221) was used to probe an ordered YAC library under low-stringency hybridization conditions as described previously (Titus et al., 1994). In brief, the DNA fragment was ^{32}P-labeled by randomly primed DNA synthesis and hybridized to Southern blots of a set of 1,016 YAC clones representing >99% of the *Dictyostelium* genome (Kuspa et al., 1992). The hybridization was carried out for 36 h at 37°C in 10 mM Tris-HCl, pH 8.0, 1 M NaCl, 5× Denhardt's solution, 0.1 mg/ml sheared salmon sperm DNA, 0.5% SDS, 30% formamide, and 10^6 cpm/ml labeled DNA. The blots were washed twice for 30 min each in 6× SSC and 0.5% SDS at 58°C and exposed to film for 4 d. After the assignment of hybridization signals to specific YAC clones, overlapping clusters of clones were assigned to specific chromosomal loci including the previously identified *abpA* (α-actinin) and *abpC* (gelation factor) loci, as well as two new loci (*abpD* and *abpE*) to which actin-binding protein genes had not been previously mapped. A YAC clone from locus *abpD* was purified from the endogenous yeast chromosomes by pulsed field gel electrophoresis (Kuspa and Loomis, 1996*a*) and used as a PCR template using degenerated primers abs-1 (5′-CAAMAAAAWACTTTYACTMRWTGG-3′) and abs-2 (5′-TAAAATWAWAKTCCAAATTAAACC-3′) corresponding to highly conserved regions of the ABD of proteins of the α-actinin superfamily (see Fig. 3 *A*). A 300-bp PCR fragment was obtained that identified a single locus in the middle of chromosome 4 (Kuspa and Loomis, 1996*b*) when hybridized to the same YAC set under standard high stringency conditions (Kuspa et al., 1992). Fig. 1 summarizes the strategy of cloning of the *abpD* gene. The 300-bp product was used as a probe to screen a genomic DNA library containing EcoRI fragments. A 2.9-kb fragment (G1) was isolated and used as starting point for isolation of four additional clones (G2 to G5) that encompassed the whole *abpD* sequence by genomic walking in the 3′ direction. In addition, screening of a λZAP cDNA library allowed the isolation of clone C5.

The DNA clones were sequenced with gene specific primers using an automated sequencer (ABI 377 PRISM, Perkin Elmer, Norwalk, CO). The Wisconsin Package Version 9.0 of the Genetics Computer Group (University of Wisconsin, Madison, WI) was used for sequence analysis.

Protein Expression and Generation of Monoclonal Antibodies

A DNA fragment encoding Met-1 to Ser-137, corresponding to part of the ABD of interaptin, was obtained by PCR using primers designed to introduce a NdeI site at the 5′ end and a BamHI site at the 3′ end. The amplified fragment was cloned into expression vector pT7-7 (Tabor and Richardson, 1992), and the recombinant protein expressed in *Escherichia coli* BL21. After lysis of the cells the recombinant protein remained in the pellet. The pellet was sequentially extracted with 2 M and 4 M urea in TEDA buffer (10 mM Tris-HCl, pH 7.8, 1 mM EGTA, 1 mM DTT, and 0.02% NaN_3). After the 4 M urea extraction the pellet was washed with PBS and used for immunization of mice.

A DNA fragment encoding Asn-954 to Gln-1158 of the rod domain, which includes one of the repetitive stretches underlined in Fig. 2, was obtained by PCR using primers designed to introduce a NdeI site and a start codon at the 5′ end and a BamHI site at the 3′ end. The amplified fragment was cloned into expression vector pET15b (Novagen, Madison, WI), and the recombinant His-tagged protein expressed in *E. coli* BL21. The product was purified from the soluble fraction of bacterial extracts on Ni^{2+}-NTA agarose (QIAGEN GmbH, Hilden, Germany) and used to immunize mice.

For mAb production BALB/c mice were immunized as described (Schleicher et al., 1984). Spleen cells were fused with PAIB3AG8I myeloma cells two days after the last boost. Hybridomas were screened for their ability to recognize the antigen on Western blots. mAb 234–151-9

recognized the ABD of interaptin, and mAb 260-60-10 recognized an epitope in the rod domain.

Strains, Growth Conditions, Development, and cAMP Stimulation of D. discoideum

Cells of *D. discoideum* strain AX2-214 (referred to as wild-type), an axenically growing derivative of wild strain NC4, and transformants were grown either in liquid nutrient medium at 21°C with shaking at 160 rpm (Claviez et al., 1982), or on SM agar plates with *Klebsiella aerogenes* (Williams and Newell, 1976). For development cells were grown to a density of 2 to 3 $\times$ 10^6 cells/ml, washed in 17 mM Soerensen phosphate buffer, pH 6.0, and 0.8 $\times$ 10^8 cells were deposited on nitrocellulose filters (Millipore type HA; Millipore, Molsheim, France) and allowed to develop at 21°C as described (Newell et al., 1969). For development in shaking suspension cells were washed as above, resuspended at 1 $\times$ 10^7 cells/ml in Soerensen phosphate buffer and shaken at 160 rpm at 21°C.

The effect of cAMP on *abpD* expression was analyzed either in suspension or on aggregated cells. For analysis in suspension, cells were starved under shaking and stimulated with 2 $\times$ 10^{-8} M cAMP pulses using a syringe attached to a perfusion pump. Cell samples were collected at regular intervals for RNA extraction and Western blot analysis. For analysis of aggregates, cells were allowed to develop on agar to the stage of tight mounds. Cells were then harvested, disaggregated by five passages through a 23-G needle and resuspended in Soerensen phosphate buffer at a density of 2 $\times$ 10^7 cells/ml. After 2 h incubation with shaking in the presence of 5 mM cAMP cells were collected for RNA extraction and Western blot analysis.

Construction of lacZ Reporter Vectors and β-Galactosidase Staining

Two promoter::*lacZ* fusions were constructed using pDdGal (Harwood and Drury, 1990) as expression vector (see Fig. 1). A 2-kb fragment was excised from genomic clone G1 by digestion with EcoRI and MunI. This fragment (L1) contained 1.8-kb of 5′ flanking sequences and 225 bp of coding sequence. Additionally, a 1.8-kb PCR fragment (L2) was obtained using clone G1 as template, and primers designed to introduce a XbaI site at the 5′ end and a EcoRI site at the 3′ end. This fragment contained 800 bp of 5′ flanking sequence and 1 kb of sequence downstream of the ATG codon, and included the first intron. Both fragments were cloned in frame with the *lacZ* gene of pDdGal and the resulting vectors were introduced into AX2 cells by electroporation (Mann et al., 1994). After selection for growth in the presence of G418 (Sigma Chemical Co., St. Louis, MO), transformants were confirmed by β-galactosidase staining. Cells were allowed to develop on nitrocellulose filters placed on 2% phosphate agar. At appropriate times filters were stained for β-galactosidase activity according to the method of Dingermann et al. (1989).

Construction of a Vector Allowing Expression of a GFP Fusion Protein

A vector was constructed that allowed expression of green fluorescent protein (GFP) fused to a COOH-terminal fragment of interaptin in *Dictyostelium* cells under the control of the actin-15 promoter and the actin-8 terminator. The cDNA fragment C5 (see Fig. 1) was cloned in frame at its 5′ end to the coding region of the red shifted S65T mutant of *Aequoria victoria* GFP in the transformation vector pDEX-GFP (Westphal et al., 1997). The continuous reading frame was composed of GFP, the heptapeptide linker KLEFGTR resulting from the cloning strategy, and an interaptin fragment from Glu-1441 to the end. The resulting vector was introduced into AX2 cells by electroporation. After selection for growth in the presence of G418 (Sigma Chemical Co.), GFP-expressing transformants were confirmed by visual inspection under a fluorescence microscope.

Disruption of the abpD Gene

For construction of an interaptin targeting vector a 0.9-kb DNA fragment was excised from clone G2 by digestion with EcoRI and SpeI, blunted with Klenow fragment and ligated into the HindIII site of pBsrΔBam (Adachi et al., 1994), previously blunted with Klenow. This plasmid was linearized with EcoRI and the 3-kb EcoRI fragment G1 was cloned. The resulting vector (see Fig. 10 *A*) was introduced into AX2 cells by electroporation. Since mAb specific for interaptin were not available at the time the mutant was generated, a PCR approach using *Dictyostelium* amoebae DNA as template (Rivero et al., 1996*b*) was used for screening after selection for growth in the presence of blasticidin (ICN Biomedicals Inc., Aurora, OH). Primers were designed that allowed amplification of a 1.1-kb DNA fragment in wild-type cells (Fig 10 *A*). Due to the insertion of the Bsr cassette, the fragment size increased to 2.5 kb, whereas the endogenous 1.1-kb fragment was absent. In ~35% of the transformants tested the *abpD* gene was knocked out.

Western, Southern, and Northern Blotting

SDS-PAGE and Western blotting were performed essentially as described previously (Laemmli, 1970; Towbin et al., 1979). Polyvinylidene difluoride (PVDF; Immobilon-P; Millipore Corp., Bedford, MA) was used as blotting matrix. Iodinated sheep anti–mouse antibodies or the enhanced chemiluminescence detection system (Amersham Pharmacia Biotech, Freiburg, Germany) were used.

DNA and RNA were isolated as described (Noegel et al., 1985), transferred onto nylon membranes (Biodyne B; Pall Filtron, Dreieich, Germany) and incubated with ^{32}P-labeled probes generated using a random prime labeling kit (Stratagene, La Jolla, CA). Hybridization was performed at 37°C for 12–16 h in hybridization buffer containing 50% formamide and 2× SSC. The blots were washed twice for 5 min in 2× SSC containing 0.1% SDS at room temperature and for 60 min in a buffer containing 50% formamide and 2× SSC at 37°C.

Fluorescence Microscopy

Cells were fixed either in cold methanol (−20°C) or at room temperature with picric acid/paraformaldehyde (15% vol/vol of a saturated aqueous solution of picric acid/2% paraformaldehyde, pH 6.0) followed by 70% ethanol. For studies on developed cells, multicellular structures were disaggregated by passage through a 23-G needle before fixation. For studies on whole mounts, multicellular structures were transferred onto glass slides and fixed for 5–10 min in methanol at room temperature. Interaptin was detected using mAb 260-60-10, protein disulfide isomerase (PDI) using mAb 221-135-1 (Monnat et al., 1997), the A subunit of the V/H^+-ATPase using mAb 221-35-2 (Jenne et al., 1998) and contact site A glycoprotein using mAb 33-249-17 (Berthold et al., 1985), followed by incubation with Cy3-labeled anti–mouse IgG (Weiner et al., 1993). Nuclei were stained with 4′,6-diamidino-2-phenylindole (DAPI; Sigma Chemical Co.).

Confocal images were taken with an inverted Zeiss LSM 410 laser scanning microscope with a 40× Neofluar 1.3 oil immersion objective. For excitation, the 488-nm argon-ion laser line was used, and the emission collected with a 510–525-nm band-pass filter. Conditions for simultaneous acquisition of GFP and Cy3 fluorescence and for image processing were as previously described (Maniak et al., 1995). Confocal images of multicellular structures were taken with an inverted Leica TCS-SP laser scanning microscope with a 16× PL Fluotar 0.5 oil immersion objective. The 568-nm krypton ion laser line was used for excitation. Images were processed using the accompanying software.

Cell Fractionation Experiments

Cells were allowed to develop for 15–18 h on nitrocellulose filters. Multicellular structures were washed off the filters, disaggregated and lysed in cold TMKS buffer (50 mM Tris-HCl, pH 7.4, 5 mM $MgCl_2$, 25 mM KCl, 250 mM sucrose) with a protease inhibitor cocktail (Boehringer Mannheim GmbH, Mannheim, Germany) by repeated passage through 5-μm Nuclepore filters (Corning Costar Corp., Cambridge, MA). Cytosolic and membrane (including nuclei) fractions were separated by ultracentrifugation at 120,000 *g* for 1 h at 4°C. For extraction experiments the pellet was further treated by gentle homogenization with either 1 M KCl or 0.1 M NaOH in TMKS buffer followed by ultracentrifugation. For fractionation experiments membrane fractions prepared as above were separated in a discontinuous sucrose gradient essentially as described by Hohmann et al. (1985). Acid and alkaline phosphatase activities were measured as described previously (Loomis, 1969; Loomis and Kuspa, 1984). For lysis in the presence of Triton X-100, lysis buffer (10 mM MES, pH 6.1, 138 mM KCl, 3 mM $MgCl_2$, 2 mM EDTA, 1% Triton X-100) was added to a cell pellet after disaggregation. The lysate was then ultracentrifuged as above.

Miscellaneous Methods

Standard molecular biology methods were as described by Sambrook et al. (1989). RT-PCR was performed using a Tth DNA polymerase kit (Boeh-

ringer Mannheim GmbH) according to the instructions supplied by the manufacturer. Cell size and resistance to osmotic shock were quantitated as previously described (Rivero et al., 1996*a*). To analyze agglutination cells were adjusted to an OD_{600} of 0.9 (roughly equivalent to a density of 1×10^7 cells/ml) in 5 ml Soerensen phosphate buffer and were shaken at 160 rpm. To follow the time course of agglutination, changes in optical density (600 nm wave length) were monitored using a LKB Ultrospec III spectrophotometer (Pharmacia Biotech Sverige, Uppsala, Sweden).

Results

Molecular Cloning of abpD

We have used a YAC-based approach to identify the *abpD* locus (Fig. 1), which has been mapped to the *Dictyostelium* chromosome 4 and codes for interaptin, an actin-binding protein of the α-actinin superfamily. The coding region of the *abpD* gene spans 5.7 kb and is interrupted by two introns. The first intron is inserted in the middle of the serine codon AGT at amino acid 173 and has two features that make it unusual for *Dictyostelium* introns: its length (417 bp) and the presence of GC-rich stretches. RT-PCR was used to confirm the intron–exon boundaries of this intron. To this end a reverse primer was designed downstream of the first intron and was used for reverse transcription of total RNA from developed cells. The resulting cDNA was used as a template for PCR using the same reverse primer and a forward primer derived from a sequence upstream of the first intron. The second intron is placed at alanine codon GCA corresponding to amino acid 1679, and is 82 bp long. cDNA clone C5 allowed confirmation of the intron–exon boundaries. The coding region is flanked by noncoding sequences containing extensive homopolymeric A+T rich stretches, as is characteristic of *Dictyostelium* intergenic regions (Kimmel and Firtel, 1983). The 5′ intergenic region is 777 bp long and contains the promoter. Several GC-rich stretches are interspersed in this region. A polyadenylation signal was found 115 bp after the stop codon. The *abpD* locus is flanked by one ORF on either side. We did not find any homology in the data bases for the ORF upstream of *abpD*. The ORF situated downstream shows homology to a variety of carboxylases.

The genomic organization of the *abpD* gene was studied by Southern blot analysis (not shown). Genomic DNA was cut with a variety of restriction enzymes and hybridized under high and low stringency conditions with probes generated along the *abpD* gene (P1 to P4). Under high-stringency conditions all probes hybridized to one or two DNA fragments, as expected from the location of restriction sites deduced from the gene sequence. Under low stringency conditions additional bands were apparent with probe P1, which contains sequences for the ABD. This result was expected, since the high similarity among the ABD of members of the α-actinin superfamily was exploited to clone *abpD*. Additional faint bands were also apparent under low stringency conditions with probes P2 to P4 in a pattern consistent with the presence of more than one related gene. Screening of a λZAP cDNA library using probe P3 under low stringency conditions yielded numerous clones corresponding to proteins all of them characterized by the presence of polyglutamine stretches. Similar stretches are present throughout the central portion of interaptin and could be responsible for the pattern observed in Southern blots under low stringency conditions. On the other hand, rescreening of the YAC library under low stringency conditions with probe P2, which is devoid of sequences for the ABD, did not reveal additional loci, indicating that *abpD* is present as a single locus.

Sequence and Structural Features of Interaptin

The *abpD* gene sequence predicts a protein composed of 1,737 amino acids, with a calculated molecular mass of 204,300 D (Fig. 2). Based on structural and functional analyses interaptin exhibits three distinct domains linked by serine-rich amino acid stretches (Fig. 3). An ABD of the α-actinin superfamily of ~250 amino acid residues is situated in the NH_2-terminal region. The sequence of this domain showed the highest identity (40.4%) to the ABD of gelation factor (ABP-120). The identity to the ABD of other members of the α-actinin superfamily like α-actinin, cortexillin, β-spectrin, dystrophin, utrophin, ABP-280, plectin, and dystonin was 33–39%, and dropped to ~20% for members of the fimbrin/plastin family (Fig. 3 *A*). Due to low solubility of a bacterially expressed peptide containing most of the ABD of interaptin, biochemical analyses of the actin-binding properties of this domain could not be performed. However, from the high degree of conservation it is likely that the ABD of interaptin is capable of binding to filamentous actin.

Structural predictions provided by the COILS algorithm (Lupas et al., 1991) define a central rod domain of 1,180

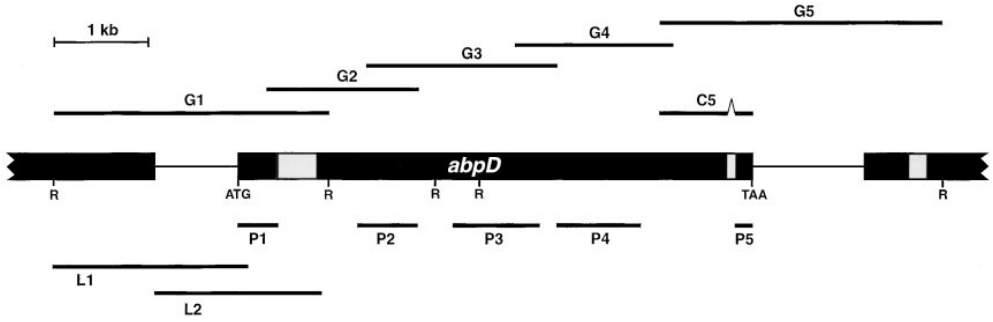

Figure 1. Strategy of cloning and genomic organization of the *abpD* gene. Five overlapping genomic clones (G1 to G5) encompassing 8.6 kb were isolated and sequenced in both directions. Additionally, a cDNA clone (C5) was obtained after screening a λZAP cDNA library. The coding sequence is interrupted by two introns (*shaded*) of 417 and 82 base pairs. The *abpD* locus has been mapped to chromosome 4 of the *Dictyostelium* genome. DNA fragments used as probes for Northern and Southern blot analyses are depicted as P1 to P5. DNA fragments used for construction of *lacZ* fusions are depicted as L1 and L2. *R*, EcoRI restriction sites.

```
MEHSTPLNEE IVHKKNDENW VIAQKKVFTN WCNIFLNQRS QKIEDLETDL    50
YDGILLGSLL EILSGKNVIL SKCKQLKTRL HYINNLNFSL KFIGDEGLRL   100
VGVASEDITD GNLKLILGLV WTLILRYQIQ SMQNSKSSQQ NLHSSTKPSE   150
LMLNWVKSQI SDYGHHIKDL TTSFQNGLLF CALVHKLVPE KLDYKSLSES   200
DSLGNLTLAF EVANKELGIP SILDPHDIIT TPDELSILTY ISLFPKVYQQ   250
TLEPLNNNNN ISPSLSSSSS SLLNTPNKRN SIQLSKSTSF EQQNQQQQQQ   300
NLLSPNSYRN SISFSKSPSF EGSQSTGSSR SISPISSPIK NSTTGNSNLS   350
KSTSFEKIEA SNTTNNNTII IAEESRVIEK IVEKIIEVEK IVEVEKIVEV   400
EKIVEVEKIV EVEKIVKVDD IEKLTNLQDQ LTEQQQQYQE KSLKLVNLEL   450
ELQEKSNQLV DKSNQLSTMQ ATNSELMEKI GGLMNDLTDI PTQDIKEKDE   500
IIANLKIESE KNLKCFQDDF NALQSRYSLT IEQTSQLQDR IKQLINELQE   550
RDDKFIEFTN SSNQSLADNQ RVIDQLTNEK QSITLQLQDQ QDIKEKEFQF   600
EKQQLLSQID SITTNIQEYQ DKFNNLQQEF NTQQTLNQQE THRLTQQLYQ   650
INTDYNEKQT QLQSEIKDNQ TINEQLNKQL SEKDKEIEKL SNQQEQQQDE   700
KINNLLLEIK EKDCLIERIN QQLLENIDLN SKYQQLLLEF ENFKLNSSKE   750
KENQLNELQS KQDERFNQLN DEKLEKEKQL QSIEDEFNQY KQQQLSSNSN   800
IDQQLQSTII ELSELKEQKE LNDSKLIEKE KQLQQLQQEF DQLNEKNQKD   850
HQDQLELLEK QLKQLQQEYD QLNETNQSIE NQLNQQNLIN KENLNEKEQE   900
LLKLQNQLNQ QIEKIQFDQQ EFSKQNSINI ELVNEKNEKL IQLQQDYDQL   950
KQQNRSNDEK DENDLIEKEN QLKSIQNELN QLIEKNESDH KEQQLKQQSI  1000
ENDLIEKENQ IQQLQSQLNE QRQQQSNQLS EKDQQLNQLI EKNQFDQKEQ  1050
QLKQQSIEND LFEKENQIQQ LQSQLNEQRQ QQSNQLSEKD QQLNQLIEKN  1100
ESDQKEQQLK QQSIENDLIE KENQIQQLQL QLNEQRQLQS EVSIDNDKIL  1150
ELEKQLKQCQ SDLLKLNDEK QQQDKQLQDK QIEFDQLQLT FNQFKNDKDS  1200
QFIQLQDDQK QQLQSIQQDL NQLKQENQEK EKQLSEKDEK LQSIQFENQE  1250
KEKQLSEKDE KLQSIQQNLN QLNDENQEKV KQFSEKDEKL QSIQQDLNQL  1300
KQENQEKEKQ LSEKDEKLQS IQQDLNQLND DQIKKNEKLK EKEEQLLKLQ  1350
QDFNDQQSQQ LKQLEEKLSE KENQLQQLKQ ENEINQLNQQ QQSNEIIQQL  1400
KDQLLKQQQQ EQQENNNEKE IERLIQEIEQ LKQQQEIDQS ELSNKEIKIQ  1450
TTQQEFDQLS HNRSKDQLHL QQLQQELDQL KQSFDQDHQF KKVIDERYNL  1500
QLQLEQSTLS NNQLDQLLKE KLKPLELDSN EKQKTIDDLL SNISNLQISL  1550
QNDKDLISER NNSIKTLESR ITQQLSLLDE KDNLIKDLQQ QKQQQQQPPT  1600
ASSSPSSSPS LLSSTPTPKP QRPNQIEIDR LVNEIVNRNQ DLIRKNKTKF  1650
YKLENGDYIV NSIIYRLSLD DDNDSDLIAQ EYENGNSTTF EKSLRIFPSK  1700
NTRPIFDWRA LFFIGAAVLA ISTLFSSSRP IKYEKPT                 1737
```

Figure 2. Deduced amino acid sequence of interaptin. The sequence predicts a protein of 204.3 kD. Internal repeats in the rod domain are underlined. A putative tyrosine phosphorylation site is boxed. A stretch of nonpolar amino acids at the COOH terminus is double underlined. Interaptin has received the GeneBank accession number AF057019.

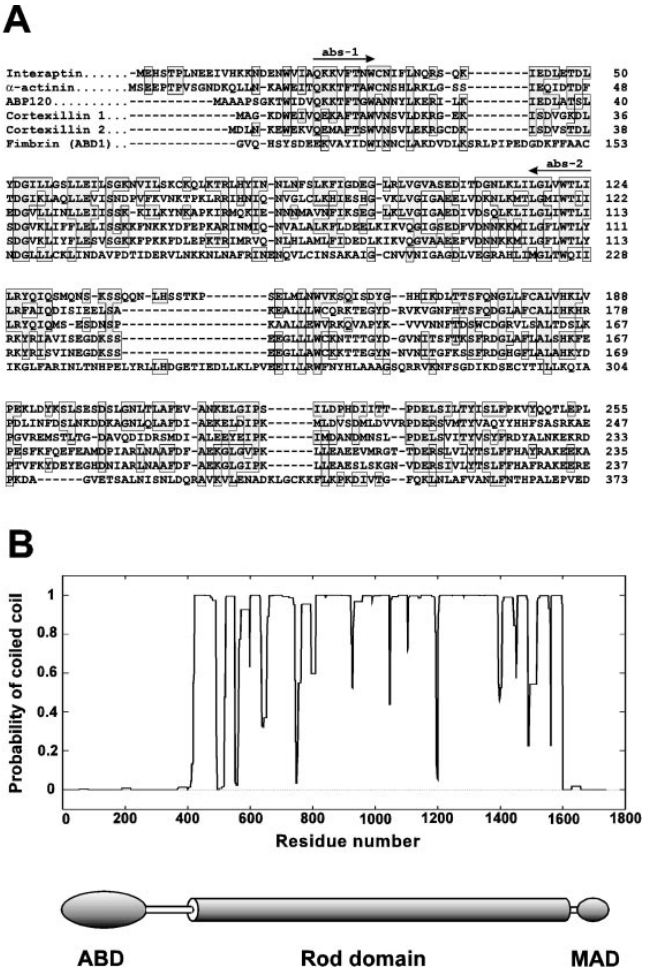

Figure 3. Structural features of interaptin. (*A*) Alignment of the ABD of interaptin with the ABD of other members of the α-actinin superfamily described in *Dictyostelium*. For fimbrin only the first ABD has been considered. The alignment was generated using the Clustal W program. Dashes indicate gaps introduced in the sequence for optimal alignment. Residues that are identical between interaptin and any of the other members of the α-actinin superfamily are boxed. Arrows indicate the sequences used to design the degenerate primers for cloning the *abpD* gene. GeneBank accession numbers: interaptin, AF057019; α-actinin, Y00689; ABP-120, X15430; cortexillin 1, L49527; cortexillin 2, L46371; fimbrin, L36202. (*B*). Probability of forming α-helical coiled-coil structures. Matrix MTIDK of the COILS version 2.1 algorithm (Lupas et al., 1991) was used with a window size of 28 and weighting. High values are reached through the central portion of the protein, defining a rod domain. The proposed structure of interaptin is shown below. The protein consists of three functional domains connected by serine rich stretches: an NH_2-terminal ABD (Met-1 to Leu-255), a central rod domain (Lys-417 to Gln-1597) and a COOH-terminal MAD (Asn-1624 to Thr-1737).

amino acids with a predominant coiled-coil α-helical structure (Fig. 3 *B*). This domain displays a particular amino acid composition, with a high content of glutamine (22.5%), leucine (14.3%), glutamic acid (12.7%), lysine (10.9%), and asparagine (9.7%). Two stretches of 179 and 117 residues (underlined in Fig. 2) are composed of four incomplete and nearly identical repeats of 57 and 28 residues, respectively, which probably arose by internal gene duplications. A putative tyrosine phosphorylation site is present at the end of the rod domain (boxed in Fig. 2), in a region of lower probability of coiled-coil structure. Search of sequence databases with the rod portion of interaptin revealed weak homology (19–24% identity; up to 49% similarity) to >50 entries corresponding to tail sequences of myosins, indicating a structural relationship, since the tails of certain myosins also possess a coiled-coil structure.

The last ~120 amino acid residues of interaptin constitute a domain involved in membrane association. Evidence on the role of this domain in determining the subcellular localization of interaptin is presented below. This domain shows a particularly high content (41.5%) of hydrophobic and nonpolar amino acid residues. A stretch of 12 consecutive hydrophobic or nonpolar residues is double-underlined in Fig. 2. No sequence homology was found between this domain and known proteins in the databases.

Developmental regulation of the abpD Gene

One prominent feature of the *Dictyostelium* life cycle is the transition from single cell amoebae to a multicellular fruiting body consisting of at least two differentiated cell types. This transition is induced by starvation of the cells and involves coordinated transcription of certain genes and differentiation and sorting out of cell populations. This process is regulated by diffusible signals and strongly depends on the integrity of the actin cytoskeleton. We have used Northern blot analysis to study the expression of the *abpD* gene during synchronized development on nitrocellulose filters. Hybridization with probes P1, P3, and P5 revealed a transcript of 5.8 kb that is expressed at very low levels during growth phase and the early aggregation period (Fig. 4 *A*). Levels of this transcript reached a maximum at 12–16 h, a stage when differentiation and sorting out into prespore and prestalk cells take place and in fact, this period of maximal expression is concomitant with expression of prespore- and prestalk-specific genes, particularly *pspA* (Fig. 10 *C*). Expression of the 5.8-kb transcript decreased to basal levels during maturation of the fruiting body. Hybridization with probes P3 and P5 revealed an additional 5.4-kb transcript that is expressed at very low levels throughout the *Dictyostelium* developmental cycle. Since this transcript was not detected by probe P1 (not shown), it appears to arise by differential splicing or by the use of a second promoter presumably located in the first intron, which displays unusual features (see above). In fact, experiments with a fusion of the first intron with a β-galactosidase reporter gene indicated that this intron can display promoter activity (unpublished). High amounts of RNA and prolonged exposure times after hybridization were necessary to detect both transcripts, indicating that expression levels are low. When *abpD* transcript accumulation was analyzed in cells starved in suspension, an increase in the 5.8-kb transcript was observed after 12 h of starvation. Levels continued to increase until at least 18 h of starvation, paralleling the behavior of the *pspA* mRNA (not shown).

Total cell homogenates of cells developed under the same conditions were analyzed using Western blotting with mAb 260-60-10. This mAb, raised against a fragment of the interaptin rod domain, recognized bands of 200 and 160 kD (Fig. 4 *B*). The 160-kD band appeared as a constitutive protein, and almost equal amounts were present throughout the entire developmental cycle, including 24 h. The 200-kD band, whose size is in agreement with the predicted molecular mass of interaptin, was present at very low levels during the early stages of development. The amount of the 200-kD protein increased during late aggregation, reached a maximum and was maintained during culmination and maturation of the fruiting body. Western blot analysis with mAb 234-151-9, raised against the ABD, recognized both the 160- and the 200-kD bands, and additionally two weak bands of ~95 and 120 kD, probably corresponding to α-actinin and ABP-120, respectively (not shown). Comparison of Fig. 4, *A* and *B* shows that the stage at which mRNA and protein levels rise are coincident. At later stages mRNA levels decrease, whereas protein levels are maintained, indicating that interaptin remains in the cell as a stable protein (see also Fig. 6). The relationship between the 200- and the 160-kD proteins and of both to the 5.8 and 5.4 transcripts is still unclear. Both proteins appear to be immunologically related and behave identical in extraction and sucrose gradient experiments (see below). Size and developmental pattern of the 200-kD band suggest that this protein is the product of the 5.8-kb transcript of the *abpD* gene, and this was confirmed by the generation of mutants in which *abpD* was knocked out (see below) or overexpressed (not shown). The origin of the 160-kD protein is not clear yet; although it could derive from the 5.4-kb transcript, its presence in the *abpD*$^-$ mutant, although at low levels, argues against the hypothesis of both proteins being encoded by the same gene.

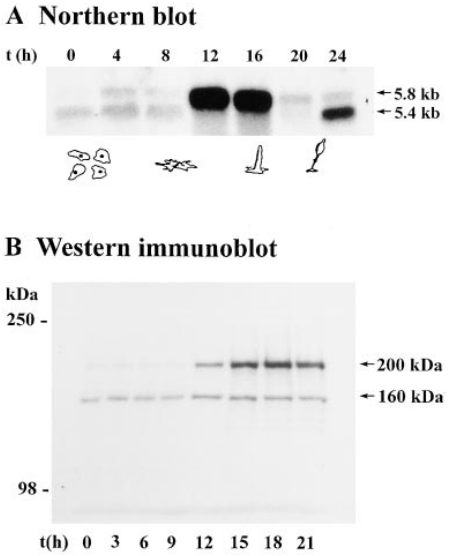

Figure 4. Developmental regulation of the *abpD* gene. *Dictyostelium* amebae were starved on nitrocellulose filters. At the indicated time points samples were taken for RNA extraction or preparation of total cell homogenates. (*A*) RNA blots containing 30 μg of RNA per lane were probed with probe P3 (see Fig. 1). Expression is highest at the mound and preculminant stage; very low levels are present at other stages of the developmental period. (*B*) Total cell homogenates of 4×10^5 cells were resolved in 6% polyacrylamide gels and blotted onto PVDF filters. Blots were incubated with mAb 260-60-10. This mAb recognizes two bands, a 160-kD constitutive band and a 200-kD developmentally regulated band.

Transcription of the abpD Gene Is Regulated by cAMP

The timing of appearance of the *abpD* transcript strongly suggested that expression of this gene might also be subject to control by cAMP. To test for cAMP dependence of transcription, cells were allowed to develop on agar to the stage of tight mounds. After stimulation of disaggregated multicellular structures with 2 mM cAMP an increase in the mRNA levels of the 5.8-kb *abpD* transcript was apparent, that paralleled the behavior of the *pspA* gene, a known cAMP-dependent late gene used as a control (Fig. 5 *A*). At the protein level an increase in the amount of the 200-kD protein recognized by mAb 260-60-10 was noted, whereas the 160-kD protein remained unchanged (Fig. 5 *B*). When tested on cells starved in suspension and stimulated with 2×10^{-8} M cAMP pulses, the *abpD* transcript

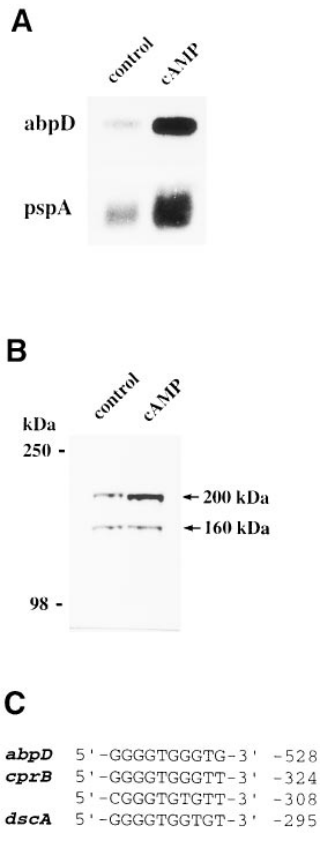

Figure 5. Expression of the *abpD* gene is regulated by cAMP. Cells were allowed to develop on agar to the stage of tight mounds, disaggregated and incubated for 2 h in suspension in the presence of 5 mM cAMP. Cells were then collected for RNA extraction and Western blot analysis. (*A*) A Northern blot containing 30 μg RNA per lane was hybridized with probe P3. For control *pspA*, a known cAMP-stimulated gene, was used. (*B*) Total cell homogenates of 4×10^5 cells were resolved in 6% polyacrylamide gels and blotted onto PVDF. Blots were incubated with mAb 260-60-10. Only the 200-kD band is stimulated by cAMP. (*C*) Comparison of G-rich sequence elements upstream of cAMP-regulated genes. Numbers indicate the position relative to the ATG start codon. *cprB*, the gene coding for cysteine proteinase 2, is cAMP inducible and contains two of these elements (Pears and Williams, 1987); *dscA*, the gene coding for discoidin 1A, is repressed by cAMP (Poole and Firtel, 1984).

appeared 3 h earlier as compared with nonstimulated cells, and was maintained at high levels at least until 18 h. A similar pattern of expression was noted for the *pspA* gene (not shown).

Many genes in *Dictyostelium* are regulated by cAMP, and the promoter regions of several of them have been studied in detail, allowing the identification of distinct GC-rich elements. The *abpD* promoter contains several regions with a high content of G + C. One of these regions is highly similar to G-rich sequence elements (GSE) of two cAMP-regulated genes: *cprB*, the gene coding for cysteine proteinase 2, that is transcribed at highest levels from late aggregation to culmination, exhibits cAMP inducible transcription and contains two GSEs arranged in tandem (Pears and Williams, 1987), and *dscA*, the gene coding for discoidin Iα, that is transcriptionally repressed by cAMP and possesses one GSE in the promoter region (Poole and Firtel, 1984; Fig. 5 *C*). Studies carried out with deletion constructs coupled to reporter genes have provided evidence for a role of GSEs in developmental and hormonal regulation of gene expression in *Dictyostelium*. Since there are several GC-rich regions in the *abpD* promoter in addition to the one referred to here, detailed analysis of this promoter is necessary to identify all control elements and establish their function.

Interaptin Is Enriched in Prestalk Cells

The pattern of regulation of the *abpD* gene suggested that accumulation of interaptin might be restricted to a particular cell type during differentiation and morphogenesis. To analyze this we carried out immunofluorescence staining with mAb 260-60-10 on whole mount preparations at different developmental stages. In slugs, intensely stained cells appeared scattered at the rear, superimposed on a homogeneous weaker staining present along the whole multicellular structure (Fig. 6 *A*). This population of intensely stained cells, which resemble in distribution the anterior-

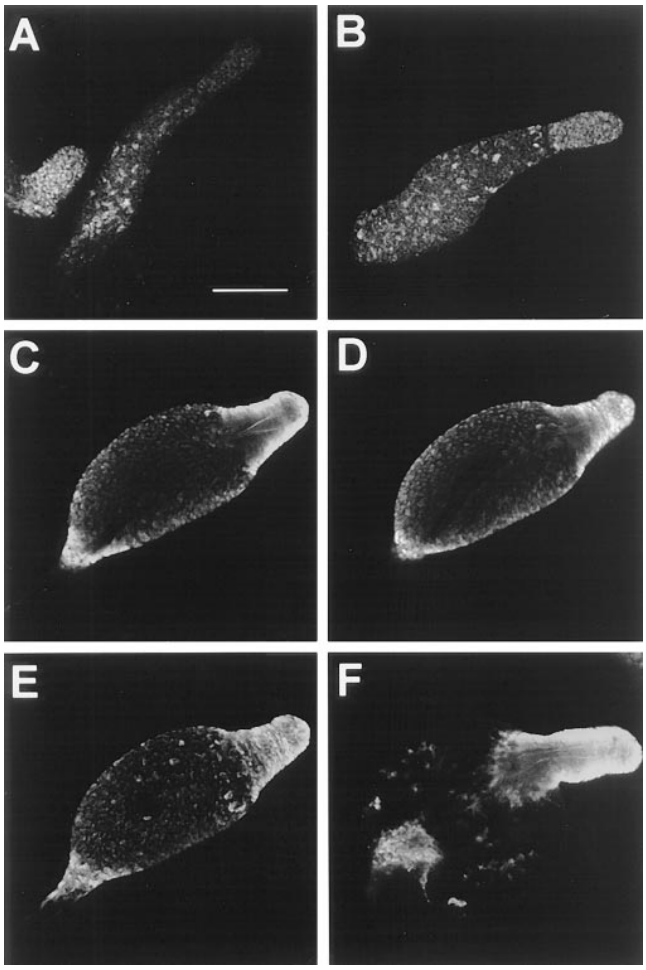

Figure 6. Investigation of cell type–specific expression of *abpD*. Cells were allowed to develop on agar, and multicellular structures were transferred to coverslips, fixed with methanol at room temperature, and then incubated with mAb 260-60-10. Optical sections were taken with a confocal laser scanning microscope. (*A*) Interaptin-rich cells appear scattered in the rear of a slug, resembling anterior-like cells. On the left, intensely stained tip of an early culminant. (*B*) Early culminant. Staining is enriched at the tip and in cells scattered along the culminant. (*C* and *D*) Two confocal sections, 16 μm apart, through a late culminant. Interaptin-rich cells accumulate at the upper and lower cups. The conus is apparent in *C*, and the stalk tube appears weakly lined by surrounding fluorescence in *D*. (*E*) Maximum projection image of a late culminant. 16 confocal sections 8 μm apart were taken. Images were superimposed and for each pixel the one with the highest intensity of all sections is represented. (*F*) Sorus of a mature fruiting body. Staining is most intense at the upper and lower cup and in few scattered cells in the spore region. Interaptin positive cells appear to line the stalk tube at the upper cup. Bar: (*A–E*) 100 μm; (*F*) 60 μm.

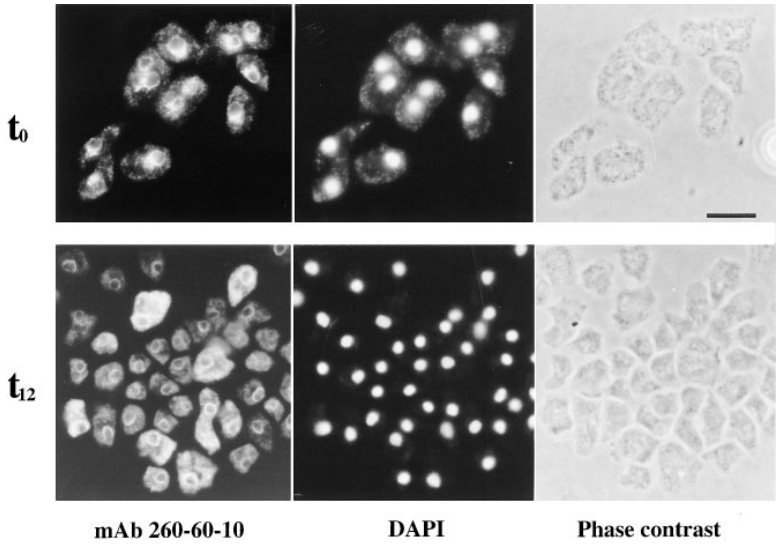

Figure 7. Immunofluorescence labeling with interaptin-specific mAb 260-60-10 of vegetative (t_0) and developed (t_{12}) cells. Developed cells were disaggregated before fixation with methanol. Perinuclear and Golgi-like staining are apparent in vegetative cells, along with a weak punctate staining throughout the cytoplasm. DAPI, a fluorescent dye that binds to DNA, was used to confirm the perinuclear localization. The same pattern is observed in developed cells, but the cytoplasmic staining is more intense in a subpopulation of cells. Bar, 10 μm.

like cells (ALC), was not apparent at previous developmental stages. Furthermore, slime trails left by migrating slugs were spotted by these strongly stained cells. As development proceeded an enrichment of interaptin was also noted at the tip of early culminants (Fig. 6 *B*, see also Fig. 6 *A*, *left*), and in late culminants and mature fruiting bodies most of the staining localized to the upper and lower cup, a behavior coincident with the fate described for the ALC (Williams, 1997), with few interaptin-rich cells still scattered in the prespore or spore region (Fig. 6, *C–F*). A funnel shaped structure at the entrance of the stalk tube was visible in late culminants (Fig. 6 *C*). Staining was absent from the stalk tube itself, which was only very weakly lined by surrounding immunostaining (Fig. 6, *D* and *F*). Beyond the sorus, the stalk and the basal disc were spotted by few interaptin-rich cells. In AX2 cells transformed with promoter::*lacZ* reporter gene constructs that contained 5′ flanking sequences of the *abpD* gene (as depicted in Fig. 1) β-galactosidase staining was observed through the whole developmental cycle, and a cell type–specific pattern was not apparent. Since β-galactosidase is characterized by its high stability, and basal *abpD* mRNA as well as protein levels are observed in vegetative cells and at early stages of development, staining at early stages masked a possible cell type–specific staining arising at later stages. Taken together, our data indicate that the *abpD* promoter directs expression of interaptin at low levels in a constitutive manner, and at high levels in a developmentally and cell type specific manner.

Subcellular Localization of Interaptin

The intracellular distribution of interaptin was studied by immunofluorescence experiments with mAb 260-60-10 on methanol fixed growth phase and developing cells (Fig. 7). Axenically grown vegetative cells display a conspicuous perinuclear staining accompanied by an intense Golgi-like staining. Additionally, a much weaker punctate staining is distributed all over the cytoplasm. For studies on developing cells slugs were mechanically dissociated before fixation. Developing cells are smaller than vegetative cells. Like these, they display a pattern of intense perinuclear and weaker cytoplasmic staining except for a population of cells (see also Fig. 6), in which a very intense staining is apparent also in the cytoplasm. Comparable results were obtained after fixation of the cells with picric acid/paraformaldehyde, although the pattern of staining was more punctate with this fixative. Since in Western blots of vegetative cells mAb 260-60-10 recognizes a more abundant 160-kD and a less abundant 200-kD protein, staining of vegetative cells should be due in part to the 160-kD protein.

The immunofluorescence pattern described above, confirmed by immunoelectron microscopy experiments (not shown), is suggestive of an association of interaptin with intracellular membranes, and is therefore unusual for an actin-associated protein. Inspection of the interaptin amino acid sequence suggested that the COOH-terminal portion of the molecule could be responsible for membrane association. To investigate the role of the COOH-terminal domain of interaptin, that we have termed MAD, we fused GFP to a COOH-terminal fragment of interaptin containing the MAD and a short portion of the rod domain. A vector allowing constitutive expression of this fusion protein was electroporated into AX2 cells and GFP-MAD–expressing cells were used in double labeling fluorescence studies. GFP-MAD–expressing cells display a pattern of prominent perinuclear and Golgi-like staining along with an intense cytoplasmic staining (Fig. 8 *A′*). This result allowed us to attribute the COOH-terminal domain of interaptin a role in membrane association. Although simultaneous immunofluorescence staining with mAb 260-60-10 (Fig. 8 *A*) showed an overall colocalization of both fluorescent signals (Fig. 8 *A″*), wild-type *Dictyostelium* cells, in contrast to GFP-MAD–expressing cells, are characterized by a comparatively more prominent perinuclear staining with mAb 260-60-10 (compare Fig. 8, *A* with *B* and also with Fig. 7). This difference might be due to competition of GFP-MAD with the endogenous 160- and 200-kD proteins for limited amounts of binding sites on the membranes.

Pericentrosomal localization of the mAb 260-60-10 antigen was confirmed using an α-tubulin-GFP expressing

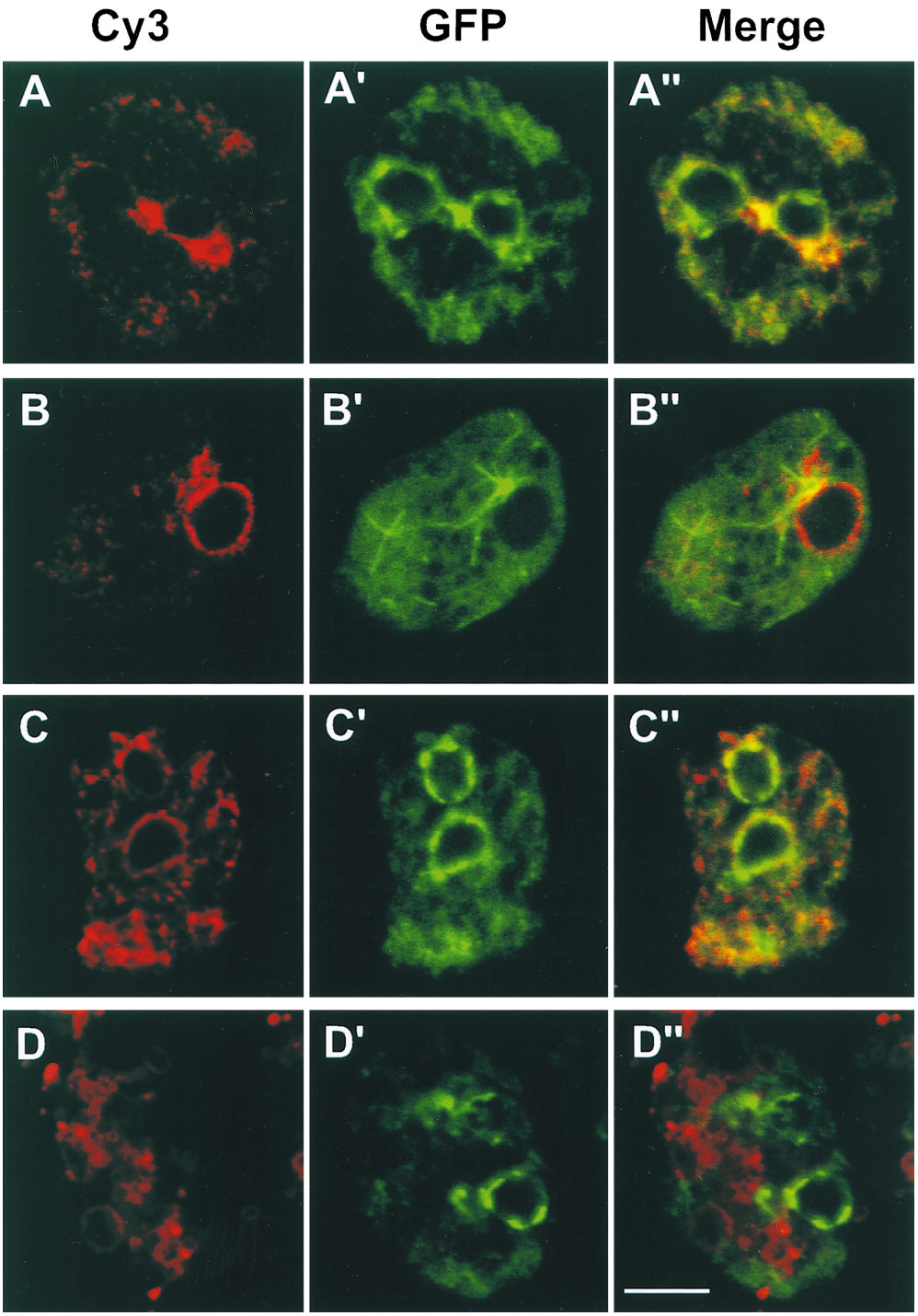

Figure 8. Subcellular localization of interaptin. Confocal sections through double labeled vegetative cells. (*A*) Immunostaining with mAb 260-60-10 of cells expressing a MAD-GFP fusion (*A′*). The merge (*A′′*) indicates that the COOH-terminal domain is responsible for the subcellular localization of interaptin. (*B*) Immunostaining with mAb 260-60-10 of cells expressing a GFP–α-tubulin fusion (*B′*). The merge (*B′′*) shows an enrichment of immunostaining in the centrosomal region. (*C*) Immunostaining with mAb 221-135-1 (an ER marker; Monnat et al., 1997) of cells expressing a MAD-GFP fusion (*C′*). (*D*) Immunostaining with mAb 221-35-2 (a marker of membranes of the contractile vacuole and the endo/lysosomal system; Jenne et al., 1998) of cells expressing a MAD-GFP fusion (*D′*). Merges *C′′* and *D′′* indicate that interaptin localizes to vesicles of the ER compartment rather than to vesicles of the contractile vacuole or the endo/lysosomal system. Bar, 5 μm.

Dictyostelium mutant (Neujahr et al., 1998). As shown in Fig. 8 *B′*, bundles of microtubules emanate from the centrosomal region of the cell. Unpolymerized α-tubulin-GFP appears as a diffuse cytoplasmic staining. Immunostaining with mAb 260-60-10 (Fig. 8 *B*) is intense around the nucleus, as well as in the pericentrosomal region (Fig. 8 *B′′*). To further identify the membrane compartments with which interaptin associates, GFP-MAD–expressing cells were labeled with mAb 221-135-1 directed against a PDI as an ER protein (Monnat et al., 1997; Fig. 8 *C*), and with mAb 221-35-2 directed against the A subunit of the V/H^+-ATPase, a protein present on membranes of the contractile vacuole and the endo/lysosomal system of *Dictyostelium* (Jenne et al., 1998; Fig. 8 *D*). Fig. 8 *C′′* shows colocalization of GFP-MAD and the ER marker. The ER appears as a tubular–vesicular meshwork distributed all over the cell and is continuous with the nuclear envelope. By contrast, the membrane compartments defined by GFP-MAD and the V/H^+-ATPase do not overlap (Fig. 8 *D′′*). Therefore, we conclude that interaptin associates with membranes of

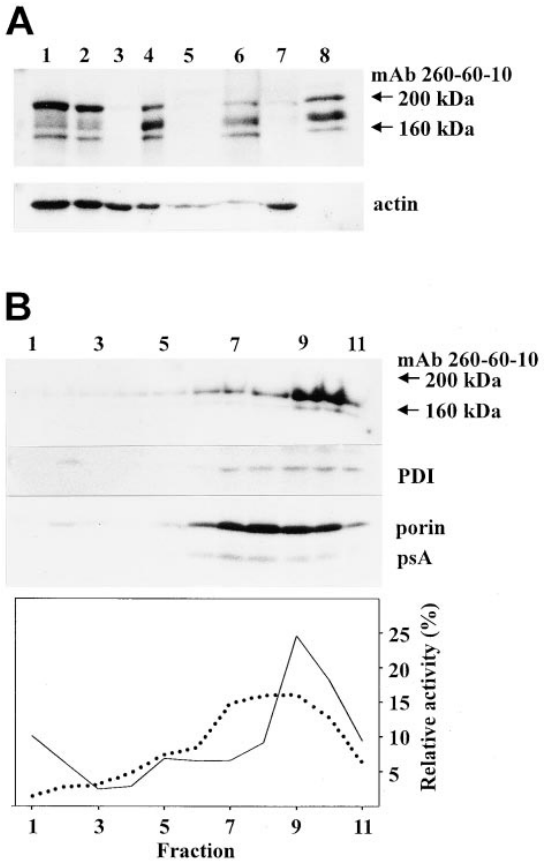

Figure 9. Extraction and subcellular fractionation experiments on developed cells. Multicellular structures equivalent to 3×10^8 cells were washed, disaggregated, lysed and processed as described in Materials and Methods. Proteins were resolved in 6 or 12% polyacrylamide gels, blotted onto PVDF and incubated with the mAbs against the proteins indicated. (*A*) Salt and alkali extraction of a membrane fraction. Lane *1*, total cell homogenate; lane *2*, total cell lysate. Lanes *3* and *4*, cytosolic and membrane (including nuclei) fraction, respectively, after 120,000 *g* centrifugation of a total cell lysate. Lanes *5* and *6*, supernatant and pellet, respectively, after extraction of the membrane fraction of lane *4* with 1 M KCl. Lanes *7* and *8*, supernatant and pellet, respectively, after extraction of the membrane fraction of lane *4* with 0.1 M NaOH. Blots were incubated with mAb 260-60-10 for interaptin and act-1 (Simpson et al., 1984) for actin. Both the 200- and the 160-kD proteins are recovered almost quantitatively in the membrane pellet after lysis and extraction with salt or alkali. The 200-kD band was partially degraded. (*B*) Sucrose gradient fractionation of a membrane (including nuclei) pellet. Samples were centrifuged to equilibrium on 30–50% (wt/vol) sucrose gradients atop 84% (wt/vol) cushions (fraction 11). After centrifugation 1 ml fractions were collected from the top and analyzed. 5–10% of each fraction was analyzed in Western blots using mAbs 260-60-10 for interaptin, 221-135-1 for PDI (an ER marker; Monnat et al., 1997), mAb100 for porin (a mitochondrial protein; Troll et al., 1992) and MUD-1 for psA (a protein of prespore vesicles; Gregg et al., 1982). The enzymes assayed were alkaline phosphatase (a marker for plasma membrane and the contractile vacuole; *dotted line*) and acid phosphatase (a marker for lysosomes; *solid line*). A fraction of the acid phosphatase has been released during the lysis step and appears at the top of the gradient. The 200-kD (almost completely degraded) and the 160-kD protein were enriched in the highest density fractions, in a pattern similar to PDI and distinct from all other markers tested.

specific intracellular compartments constituted by the nuclear envelope and the ER.

Interaptin Is Associated with Intracellular Membranes

The association of interaptin with intracellular membranes suggested by the immunofluorescence studies was further investigated in extraction experiments on developed cells (Fig. 9 *A*). After lysis by passage through Nuclepore filters, both the 160- and the 200-kD proteins were quantitatively recovered in the membrane pellet. Further treatment of this pellet with high salt (1 M KCl) or with alkali (0.1 M NaOH) did not result in extraction of significant amounts of any of the proteins, indicating a very strong membrane association. Approximately 50% of the actin cosedimenting with membranes was extracted with 1 M KCl, whereas no actin remained in the membrane pellet after treatment with alkali. When cells were lysed in the presence of Triton X-100 both the 160- and the 200-kD proteins were solubilized; under these conditions the 200-kD band was rapidly degraded to slightly smaller fragments (not shown).

To confirm the results obtained in the immunolocalization experiments presented above, we performed fractionation experiments of a membrane pellet (including nuclei) of developed cells in a discontinuous sucrose gradient. The resulting fractions were analyzed in Western blots using a panel of mAbs directed against distinct cellular compartments (Fig. 9 *B*). Probing with mAb 260-60-10 indicated that the 200-kD protein (almost completely degraded despite the use of protease inhibitors) as well as the 160-kD protein were enriched in the highest density fractions, where nuclei were also present. A similar distribution pattern was noted for PDI, a protein of the ER, and for comitin, a Golgi- and vesicle-associated protein (Weiner et al., 1993; not shown). Mitochondria, monitored by mAb100 against porin, a protein of the mitochondrial outer membrane (Troll et al., 1992), peaked at fractions 8 and 9, and psA, a protein present in prespore vesicles (Gregg et al., 1982), is apparent in fractions 7–10. Furthermore, the distribution pattern observed with mAb 260-60-10 was also distinct from the distribution of the enzyme markers alkaline phosphatase, a marker for plasma membrane and the contractile vacuole, and acid phosphatase, a marker for lysosomes.

Generation of an abpD⁻ Mutant

To gain insight into the function of interaptin we have generated an *abpD*⁻ mutant by homologous recombination. To this end we made a construct in which the blasticidin (Bsr) resistance cassette was inserted in an ~4-kb genomic fragment of the *abpD* gene, between the sequences coding for the ABD and the linker to the rod domain (Fig. 10 *A*). Southern blot analysis was used to characterize the recombination event (Fig. 10 *B*). The results allowed us to conclude that a gene disruption event had occurred in the *abpD*⁻ mutant. The deduced genomic organization of the disrupted gene is depicted in Fig. 10 *A*. Northern blot analysis confirmed the absence of transcripts derived from the *abpD* gene in the mutant, whereas the Bsr resistance gene was expressed (Fig. 10 *C*). In Western blot analysis with mAb

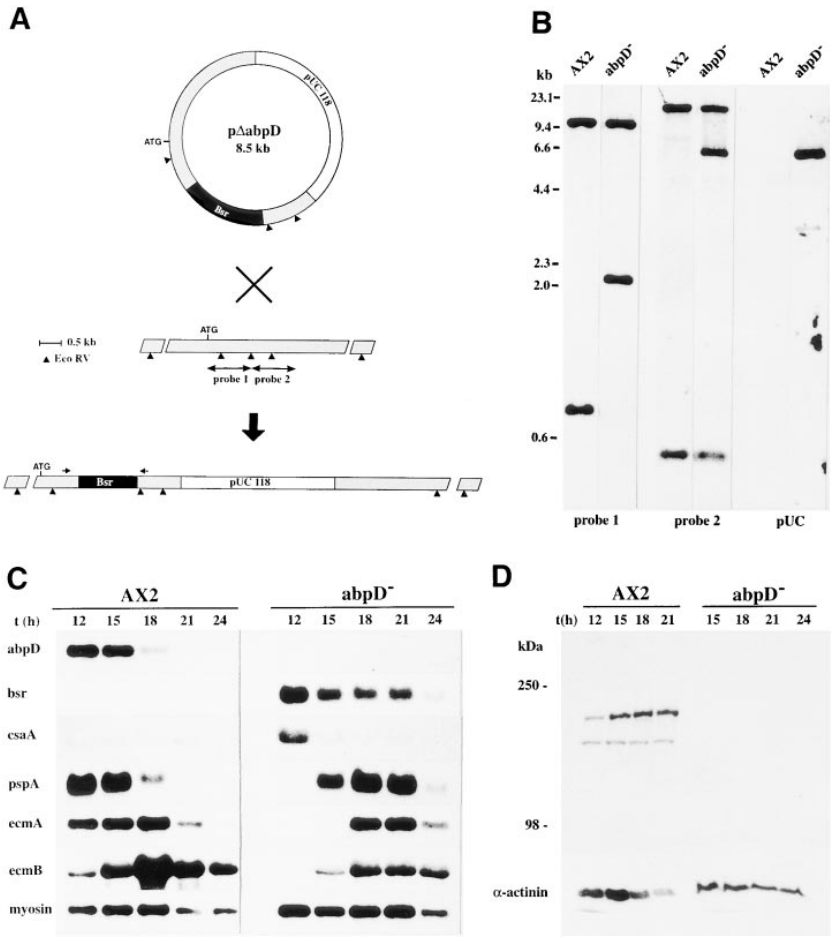

Figure 10. Generation of an *abpD*$^-$ mutant by homologous recombination. (*A*) A construct was made in which the blasticidin resistance cassette (Bsr) was inserted in a genomic clone between the ABD and a portion of the rod domain. The arrows at the bottom indicate the position of the oligonucleotide primers used for the PCR screening of mutants. (*B*) Southern blot analyses demonstrate that a gene disruption event has occurred. Genomic DNA was digested with EcoRV and blots probed with the ^{32}P-labeled DNA fragments indicated below. With probe 1 insertion of the Bsr cassette causes the shift of a 0.75-kb band to a 2.2-kb band in the mutant. With probe 2 an additional band of ~6 kb is apparent in the mutant which contains sequences of the pUC118 transformation vector, as shown after hybridization with a pUC probe. (*C* and *D*) Development of *abpD*$^-$ mutant. AX2 and mutant cells were allowed to develop on nitrocellulose filters. At the indicated time points samples were taken for RNA extraction and Western blot analysis. Northern blots containing 30 μg RNA per lane (*C*) were probed with probe P1 to demonstrate that no RNA message is present in the mutant, whereas the blasticidin resistance gene (*bsr*) is expressed. Similar result was obtained with probe P4. Blots were also hybridized with probes for developmentally regulated genes. *csaA* codes for the cell adhesion molecule contact site A, responsible for cell–cell contacts in early aggregates (Noegel et al., 1986). *pspA* encodes the prespore-specific cell surface protein psA (Early et al., 1988). *ecmA* and *ecmB* encode the prestalk-specific extracellular matrix proteins ST340 and ST310, respectively (Jermyn et al., 1987). Myosin is a control for comparable loading. The *abpD*$^-$ mutant shows a delay of ~3 h in the developmental pattern as compared with wild type. In Western blot analysis (*D*) the 200-kD band is absent, and the 160-kD band appears as an extremely faint band in the *abpD*$^-$ mutant. The blot was subsequently probed with α-actinin–specific mAb 47-62-17 (Schleicher et al., 1988) to show comparable loading.

260-60-10 absence of the developmentally and cAMP-regulated 200-kD protein that we identify with interaptin was noted. The 160-kD protein was present as a very faint band, apparent only after long exposure of the autoradiogram (Fig. 10 *D*). Furthermore, in immunofluorescence studies with mAb 260-60-10 on growth phase *abpD*$^-$ cells, only a weak discontinuous perinuclear staining could be observed which should be due to the presence of the 160-kD protein. It appears that the 160-kD protein becomes instable in the absence of interaptin, suggesting a functional relationship between both proteins.

abpD$^-$ *Cells Are Delayed in Their Developmental Program and Display an Adhesion Defect*

Since in wild-type cells basal levels of the 200-kD interaptin are present in vegetative cells, studies of the *abpD*$^-$ mutant were extended to growth phase cells. Growth of *abpD*$^-$ cells both in axenic medium, in suspension with *E. coli* and on a bacterial lawn was comparable to wild type. No differences were appreciated in the size of mutant cells when compared with AX2, and application of an osmotic stress did not result in an altered viability of *abpD*$^-$ cells. However, when the developmental pattern of mutant cells on a solid substratum (agar or nitrocellulose filters) was examined, a 3–4-h delay was consistently observed. The morphology of multicellular structures was unimpaired, and mature normal-looking fruiting bodies were formed (not shown). We next examined in detail the timing and levels of expression of developmentally regulated genes that are specifically expressed during aggregation (contact site A or *csaA* gene) and during cell type differentiation (*pspA* as prespore-specific marker and *ecmA* and *ecm*B as prestalk-specific markers). Apart from a delay in the onset of development, no remarkable differences in the levels of expression of these genes were observed with the exception of the *ecmB* gene, which showed lower levels of transcripts in the *abpD*$^-$ mutant than in control cells (Fig. 10 *C*).

When suspensions of *abpD*$^-$ cells were shaken for more than 12 h in Soerensen phosphate buffer, only very loose aggregates were formed, and the pale yellowish staining characteristic of AX2 cells due to pigment molecules accumulating in cell aggregates did not develop. Therefore, we examined if lack of interaptin had an effect on the ability of cells to aggregate. For this we monitored the time course of agglutination of *abpD*$^-$ cells in shaking suspen-

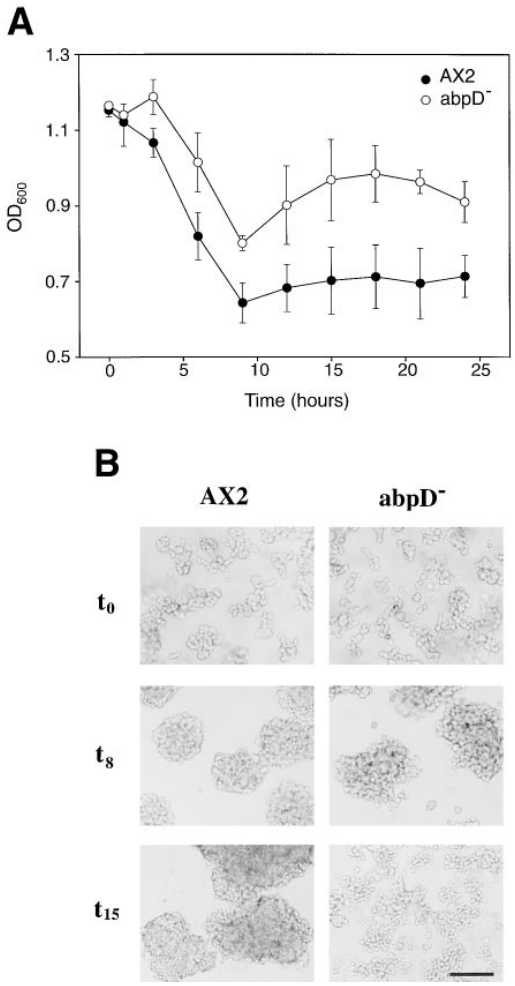

Figure 11. Alterations in the pattern of agglutination of the *abpD*$^-$ mutant. Axenically grown AX2 and *abpD*$^-$ cells were washed and starved in Soerensen's phosphate buffer at a density of 1×10^7 cells/ml with shaking at 160 rpm. At the time points indicated optical density (600 nm wave length) was measured in a spectrophotometer (*A*). Each point represents the average ± SD of three independent experiments. The pattern observed in the mutant after 9 h of starvation indicates a dissociation of the aggregates previously formed as shown in the photographs (*B*), and occurs at the time when the *abpD* gene begins to be expressed. Differences between AX2 and *abpD*$^-$ cells were significant ($P < 0.001$, Student's *t* test) from 3 h on. Bar, 100 μm.

sion by measuring the decrease in light scattering at 600 nm (Fig. 11 *A*). Under these conditions, aggregates are formed that recapitulate many of the developmental events that occur on a solid surface (Takeuchi et al., 1988). Although slightly delayed, mutant cells were able to agglutinate and build multicellular aggregates similar to the wild-type strain, as revealed by examination under the microscope after 8 h of starvation (Fig. 11 *B*). In agreement with this, Western blotting and immunofluorescence analyses did not reveal differences between both strains in the amount of contact site A glycoprotein, which is responsible for EDTA-stable cell–cell contacts in early aggregation (Noegel et al., 1986; not shown). When shaking was prolonged, aggregates of AX2 cells became larger, whereas *abpD*$^-$ aggregates dissociated, as shown in the pictures taken after 15 h. This suggests that an adhesion mechanism that is switched on at later stages of development is affected by lack of interaptin.

Discussion

A New Member of the α-Actinin Superfamily

We have taken advantage of the wide distribution and the high degree of conservation of the ABD that characterizes the members of the α-actinin superfamily of cytoskeletal proteins to identify interaptin in *D. discoideum*. Based on analyses of the amino acid sequence, three regions can be distinguished in the interaptin molecule that are connected by serine-rich linking peptides: an NH_2-terminal ABD, a central coiled-coil rod domain and a COOH-terminal MAD. Like interaptin, all other members of the α-actinin superfamily are characterized by a modular organization (Matsudaira, 1991). According to the disposition and structure of the different modules, all members can be subgrouped into four classes. Members of the fimbrin/plastin class are characterized by a tandem arrangement of two ABD preceded by a pair of EF-hands that allows for calcium regulation. A second class of proteins comprises α-actinin, spectrin, and dystrophin (as well as utrophin, the autosomal homologue of dystrophin). They are characterized by a rod domain consisting of triple α-helical repeat segments (Yan et al., 1993) that allow antiparallel dimerization, and by the presence of EF-hands. Members of a third class of proteins, constituted by the gelation factor (ABP-120) and filamin (ABP-280) possess a rod domain composed of segments of β-sheet structure arranged in an immunoglobulin-like folding (Fucini et al., 1997).

Finally, a fourth class is constituted by proteins whose rod domains have a coiled-coil conformation. In this conformation consecutive heptads of amino acid residues adopt an α-helical structure with a particular distribution of charged and nonpolar residues, allowing interaction of two or more of these coiled-coil regions, usually in a parallel arrangement (Lupas et al., 1991). Besides interaptin reported here, two other proteins of this class, cortexillin I and II, have been described in *Dictyostelium* (Faix et al., 1996). Cortexillins are able to form parallel dimers by virtue of the coiled-coil domain, which confers the molecule the appearance of a small double headed myosin. Additionally, cortexillin I possesses a putative phosphatidylinositol (4,5) bisphosphate (PIP2) recognition site, probably responsible for the cortical distribution of this protein. Plectin and dystonin have been described recently in mammalian cells (Brown et al., 1995; Liu et al., 1996). Dystonin is the neural isoform of the previously described bullous pemphigoid antigen 1 (BPAG-1), an isoform lacking an ABD. Plectin and dystonin have a similar domain structure, with an NH_2-terminal globular domain that contains the ABD, a central coiled-coil rod domain and a COOH-terminal domain constituted by globular repeats related to the ones present in the desmosomal proteins desmoplakin and envoplakin (Fuchs and Cleveland, 1998). Both proteins have also the capacity to bind simultaneously to actin filaments and intermediate filaments, localize to hemidesmosomes and contribute to mechanical

resistance of the cell. Although data on the oligomerization of interaptin as well as plectin and dystonin are not yet available, members of this class appear to constitute bifunctional links, directly connecting actin networks to other intracellular structures like membrane compartments in the case of interaptin.

A Developmentally and cAMP-regulated Actin-binding Protein

The contribution of cytoskeletal proteins to the developmental program of *Dictyostelium* has been well established by mutant analysis. The cytoskeletal proteins themselves are in general not strongly regulated during development (Noegel and Luna, 1995). Interaptin constitutes a remarkable exception, its message being expressed at highest levels at a decisive stage of the developmental cycle, namely when differentiation and sorting of prespore and prestalk cell populations to multicellular structures takes place, clearly suggesting a stage-specific role for this protein. Protein levels are also developmentally regulated, but whereas mRNA levels rapidly decrease before culmination, the protein is still present at high levels. A similar phenomenon has been reported for ponticulin, an integral membrane protein that links the plasma membrane to the underlying actin cortex in *Dictyostelium*. Ponticulin transcript levels decrease dramatically after aggregation, whereas the protein remains present, although at lower levels (Hitt et al., 1994).

Regulation by hormone-like signaling molecules, like cAMP in the case of interaptin, is also an unusual feature for a cytoskeletal protein. Cyclic AMP plays an essential role during the *Dictyostelium* life cycle. In addition to its function as chemoattractant, cAMP also regulates the expression of almost all classes of developmentally regulated genes, either directly or through stimulation of DIF (differentiation inducing factor), another *Dictyostelium* morphogen (for a review see Verkerke-van Wijk and Schaap, 1997). Cyclic AMP pulses in the nanomolar concentration stimulate expression of genes involved in aggregation, like *csaA* (csA glycoprotein) and *carA* (a cAMP receptor subtype), while repressing growth phase genes. At a later stage during aggregation, low concentration cAMP pulses induce expression of so-called early and intermediate genes like *cprB* (cysteine proteinase 2), *pde* (phosphodiesterase), *rasD* (a small G protein), and *lagC* (an adhesion molecule, see below). After aggregates have formed, micromolar concentrations of cAMP accumulate, leading to expression of prespore specific genes, like *pspA*, as well as non–cell-specific genes. Cyclic AMP also stimulates synthesis of DIF, which in turn induces expression of the prestalk genes *ecmA* and *ecmB*.

The *abpD* gene appears to display a bimodal pattern of expression that probably relies on promoter features that remain to be elucidated. On the one hand, the *abpD* gene is expressed at low levels in a constitutive manner. This is based on immunofluorescence studies on whole mounts, in which perinuclear staining with mAb 260-60-10 was apparent at all developmental stages, and on results obtained with promoter::*lacZ* reporter gene fusions. Superimposed to this basal pattern of expression, on the other hand, the *abpD* gene is expressed at high levels in a strictly regulated manner, as demonstrated in Northern and Western blot analyses, as well as in immunofluorescence studies on whole mounts. In this case interaptin is enriched in a distinct population of cells first detectable at the slug stage. According to the distribution and behavior of these cells, we identify them with so-called ALC, a sub-type of prestalk cells first described as neutral red-staining cells scattered in the prespore region of the slug (Sternfeld and David, 1981). The interaptin-rich cells, initially present at the rear of the slug, appear to migrate to the front and to the base as culmination proceeds. At the front they form part of the upper cup, and do not seem to enter the stalk tube and differentiate into stalk cells. At the base they are lifted up the stalk adherent to the spore mass, and constitute the lower cup, a structure of very variable size. Few interaptin-rich cells appear to be left behind at the basal disc and attached to the stalk during culmination. In general, ALC constitute a heterogeneous cell population, and the gene expression patterns of these and other prestalk subtypes have been extensively studied (Williams 1997). The fate of the interaptin-rich cells described here remains to be established in terms of expression of well known prestalk markers like *ecmO*, *ecmA*, and *ecmB*, that are expressed in distinct subpopulations of ALC. In any case, the *abpD* gene constitutes a marker of potential use for future studies of morphogenetic events in *Dictyostelium*.

Interaptin as a Link between Membrane Compartments and the Actin Cytoskeleton

We present immunological and biochemical evidence that interaptin is strongly associated with intracellular membrane compartments. The existence of interactions of membranes in general with actin networks and cables is well established, and they have been shown to participate in a variety of cell functions. Associations of the plasma membrane to the underlying cytoskeleton contribute to the cell shape by providing mechanical strength, and at sites of interaction with the extracellular matrix they participate in signal transduction pathways (Hitt and Luna, 1994; Cowin and Burke, 1996). In mammalian cells examples of actin-binding proteins involved in anchoring the plasma membrane to the cortical cytoskeleton are provided by spectrin and dystrophin (see Introduction). In *Dictyostelium* a number of actin-binding proteins like ponticulin (Hitt et al., 1994), hisactophilins (Scheel et al., 1989), and talin (Kreitmeier et al., 1995) could fulfill this function. For cortexillins the exact nature and the significance of the cortical distribution apparent in immunofluorescence studies is presently unknown (Faix et al., 1996). Finally, myosin Is can bind to the plasma membrane through a polybasic COOH-terminal domain, where they are proposed to contribute to the overall cortical tension of the cell (Uyeda and Titus, 1997).

On the other hand, association of intracellular membrane compartments with the actin cytoskeleton has been implicated in intracellular traffic as well as in endo- and exocytotic processes. Here actin provides the tracks for attaching vesicles and directing their transport within the cell (Kuznetsov et al., 1992). Apart from interaptin, only one example of a vesicle-associated actin-binding protein is known in *Dictyostelium*. The 24-kD protein comitin is

located on Golgi and vesicle membranes (Weiner et al., 1993), and it has been proposed that comitin links membrane vesicles to the actin cytoskeleton via mannose residues (Jung et al., 1996). This lectin-like activity would enable comitin to bind specifically intracellular membranes carrying glycoconjugates on their cytoplasmic faces. Actin-based motors are involved in organelle movement, and several classes of unconventional myosins, particularly of classes I, V, and VI, have been implicated in vesicular trafficking (reviewed in Mermall et al., 1998). More recently a nonmuscle myosin II has been described to associate with vesicles budding off the *trans*-Golgi network in mammalian cell lines, but its role is still uncertain (Ikonen et al., 1997; Müsch et al., 1997). In *Dictyostelium,* myosin II heavy chain null mutants are characterized by defective intracellular particle movement (Wessels and Soll, 1990). On the contrary, data available on *Dictyostelium* myosin Is indicate that they do not play a role in the intracellular trafficking of vesicles. Their function seems to be restricted to the phases of the endo- and exocytotic processes that take place at the cell cortex (Uyeda and Titus, 1997).

Two cytoskeletal proteins of the α-actinin superfamily have been reported to associate with intracellular membranes in higher eukaryotes, where they might play distinct roles. A homologue of erythrocyte β-spectrin colocalizes with membranes of the Golgi complex in a variety of cell types, from which it reversibly dissociates during mitosis and upon treatment with brefeldin A, a drug that perturbs Golgi structure (Beck et al., 1994). This spectrin isoform supposedly contributes to the structural integrity of the Golgi complex in a manner similar to its action at the erythrocyte plasma membrane, and in fact, an ankyrin isoform, a protein that links spectrin to the cytoplasmic domains of specific integral membrane proteins, has also been identified in the Golgi complex (Beck et al., 1997). ABP-280, on the other hand, binds to and is required for efficient sorting of furin, a transmembrane endoprotease implicated in proteolytic maturation of many proproteins within the *trans*-Golgi network/endosomal system, and is required for correct localization of late endosomes and lysosomes (Liu et al., 1997). For interaptin we have shown that the COOH-terminal domain is responsible for interaction with intracellular membranes. We have also shown that interaptin binds to membranes of distinct compartments, mainly the ER. Since interaptin lacks a motor domain, as is the case for proteins like myosin, kinesin, and dyenin that are involved in vesicle trafficking, this protein could play a structural role and contribute to the integrity and correct localization of vesicles along the secretory pathway. Alternatively, interaptin could contribute to the correct folding and/or targeting of membrane proteins by affecting their clustering with either themselves or with other membrane proteins, as has been shown for the Golgi spectrin-ankyrin skeleton (Devarajan et al., 1997) and for PDZ domain proteins (Craven and Bredt, 1998).

Experiments on agglutination of *abpD*$^-$ cells suggest a defect in a specific cell adhesion system. At least four adhesion systems are responsible for ensuring multicellularity in *Dictyostelium* and three cell adhesion molecules have been identified so far. DdCAD-1 (gp24), a calcium-binding glycoprotein with some similarity to E-cadherin, mediates EDTA/EGTA-sensitive adhesion and accumulates during the first four hours of development (Wong et al., 1996). The contact site A glycoprotein (gp80) mediates the EDTA-resistant adhesion during the aggregation stage (Noegel et al., 1986). This adhesion system is not substantially impaired in the *abpD*$^-$ mutant. Finally, gp150 is responsible for EDTA-resistant contacts during the postaggregation stage, and there is evidence indicating that this protein is encoded by the *lagC* gene (Dynes et al., 1994). Two features make this glycoprotein a potential candidate to explain the phenotype of *abpD*$^-$ cells. First, like *abpD*, the *lagC* gene is cAMP-regulated. And second, gp150 is expressed at moderate levels during cell aggregation, and rapidly accumulates in the late postaggregation stage, where it seems to constitute the last and only adhesion molecule expressed, since *lagC*$^-$ cells arrest at the loose mound stage (Dynes et al., 1994). However, *abpD*$^-$ cells are able to develop to the fruiting body stage. Therefore, it is possible that a functionally altered but still active adhesion molecule is synthesized in our mutant. Glycosylation is one of the most common forms of posttranslational protein modification and takes place in the ER and in the Golgi apparatus. One possible explanation for the mutant phenotype would be that lack of interaptin brings about an altered trafficking of vesicles from the ER to the Golgi apparatus, disturbing maturation of glycoproteins.

In summary, we describe a new actin-binding protein of the α-actinin superfamily. Like all members of this superfamily, interaptin has a modular organization and is structurally related to cortexillins, plectin and dystonin through its central coiled-coil rod domain. Additionally, interaptin possesses a novel domain for association with membranes of the ER. This specific feature, combined with the fact that interaptin is expressed mainly at a late stage in the *Dictyostelium* developmental cycle are suggestive of a specific role in membrane trafficking at this stage.

We thank L. Graciotti and J. Köhler for assistance during cloning and Dr. M. Schleicher for discussion and Dr. W. Loomis for providing a λZAP library. We are grateful to Dr. G. Gerisch for mAbs against *Dictyostelium* porin, to R. Neujahr for α-tubulin GFP–expressing cells, to M. Westphal for supplying the red-shifted GFP mutant gene, and to Dr. M. Maniak for mAbs against *Dictyostelium* PDI and V/H$^+$-ATPase A subunit. We thank R. Albrecht, J.-M. Schwartz and J. Murphy for help in the use of the confocal microscope and image processing. We are especially grateful to Dr. M. Stewart for guidance on structural features of interaptin.

This work was supported by the Deutsche Forschungsgemeinschaft No. 113/5-5, European Union grant CHRX-CT93-0250, Project grant no. 40 from the Zentrum für Molekulare Medizin Köln and National Institutes of Health Grant GM52359.

Received for publication 8 April 1998 and in revised form 22 June 1998.

References

Adachi, H., T. Hasebe, K. Yoshinaga, T. Ohta, and K. Sutoh. 1994. Isolation of *Dictyostelium discoideum* cytokinesis mutants by restriction enzyme-mediated integration of the blasticidin S resistance marker. *Biochem. Biophys. Res. Commun.* 205:1808–1814.

Beck, K.A., J.A. Buchanan, V. Malhotra, and W.J. Nelson. 1994. Golgi spectrin: identification of an erythroid β-spectrin homolog associated with the Golgi complex. *J. Cell Biol.* 127:707–723.

Beck, K.A., J.A. Buchanan, and W.J. Nelson. 1997. Golgi membrane skeleton: identification, localization and oligomerization of a 195 kD ankyrin isoform associated with the Golgi complex. *J. Cell Sci.* 110:1239–1249.

Berthold, J., J. Stadler, S. Bozzaro, B. Fichtner, and G. Gerisch. 1985. Carbohydrate and other epitopes of the contact site A glycoprotein of *Dictyostelium discoideum* as characterized by monoclonal antibodies. *Cell Differ.* 16:187–202.

Bennett, H., and J. Condeelis. 1988. Isolation of an immunoreactive analogue of brain fodrin that is associated with the cell cortex of *Dictyostelium* amoebae. *Cell Motil. Cytoskel.* 11:303–317.

Brown, A., G. Bernier, M. Mathieu, J. Rossant, and R. Kothary. 1995. The mouse *dystonia musculorum* gene is a neural isoform of bullous pemphigoid antigen 1. *Nature Genet.* 10:301–306.

Campbell, K.P. 1995. Three muscular dystrophies: loss of cytoskeleton-extracellular matrix linkage. *Cell.* 80:675–679.

Claviez, M., K. Pagh, H. Maruta, W. Baltes, P. Fisher, and G. Gerisch. 1982. Electron microscopic mapping of monoclonal antibodies on the tail region of *Dictyostelium* myosin. *EMBO (Eur. Mol. Biol. Organ.) J.* 1:1017–1022.

Cowin, P., and B. Burke. 1996. Cytoskeleton-membrane interactions. *Curr. Opin. Cell Biol.* 8:56–65.

Craven, S.E., and D.S. Bredt. 1998. PDZ proteins organize synaptic signalling pathways. *Cell*. 93:495–498.

Devarajan, P., P.R. Stabach, M.A. de Matteis, and J.S. Morrow. 1997. Na,K-ATPase transport from endoplasmic reticulum to Golgi requires the Golgi spectrin-ankyrin G119 skeleton in Madin Darby canine kidney cells. *Proc. Natl. Acad. Sci. USA*. 94:10711–10716.

Dingermann, T., N. Reindl, H. Werner, M. Hildebrandt, W. Nellen, A. Harwood, J. Williams, and K. Nerke. 1989. Optimization and in situ detection of *Escherichia coli* β-galactosidase gene expression in *Dictyostelium discoideum*. *Gene.* 85:353–362.

Dynes, J.L., A.M. Clark, G. Shaulsky, A. Kuspa, W.F. Loomis, and R.A. Firtel. 1994. *LagC* is required for cell-cell interactions that are essential for cell-type differentiation in *Dictyostelium*. *Genes Dev.* 8:948–958.

Early, A.E., J.G. Williams, H.E. Meyer, S.B. Por, E. Smith, K.L. Williams, and A.A. Gooley. 1988. Structural characterization of *Dictyostelium discoideum* prespore-specific gene D19 and of its product, cell surface glycoprotein PsA. *Mol. Cell. Biol.* 8:3458–3466.

Faix, J., M. Steinmetz, H. Boves, R.A. Kammerer, F. Lottspeich, U. Mintert, J. Murphy, A. Stock, U. Aebi, and G. Gerisch. 1996. Cortexillins, major determinants of cell shape and size, are actin-bundling proteins with a parallel coiled-coil tail. *Cell*. 86:631–642.

Fuchs, E., and D.W. Cleveland. 1997. A structural scaffolding of intermediate filaments in health and disease. *Science*. 279:514–519.

Fucini, P., C. Renner, C. Herberhold, A.A. Noegel, and T.A. Holak. 1997. The repeating segments of the F-actin cross-linking gelation factor (ABP-120) have an immunoglobulin-like fold. *Nature Struct. Biol*. 4:223–230.

Gallagher, P.G., and B.G. Forget. 1993. Spectrin genes in health and disease. *Semin. Hematol*. 30:4–21.

Goldsmith, S.C., N. Pokala, W. Shen, A.A. Fedorov, P. Matsudaira, and S.C. Almo. 1997. The structure of an actin-cross-linking domain from human fimbrin. *Nature Struct. Biol*. 4:708–712.

Grady, R.M., H. Teng, M.C. Nichol, J.C. Cunningham, R.S. Wilkinson, and J.R. Sanes. 1997. Skeletal and cardiac myopathies in mice lacking utrophin and dystrophin: a model for Duchenne muscular dystrophy. *Cell*. 90:729–738.

Gregg, J.H., M. Krefft, A. Haas-Kraus, and K.L. Williams. 1982. Antigenic differences between prespore cells of *Dictyostelium discoideum* and *Dictyostelium mucoroides* using monoclonal antibodies. *Exp. Cell Res*. 142:229–233.

Hammonds, R.G. 1987. Protein sequence of DMD gene is related to actin-binding domains of alpha-actinin. *Cell.* 51:1.

Harwood, A.J., and L. Drury. 1990. New vectors for expression of the *E. coli lacZ* gene in *Dictyostelium*. *Nucleic Acids Res.* 18:4292.

Hitt, A.L., and E.J. Luna. 1994. Membrane interactions with the actin cytoskeleton. *Curr. Opin. Cell Biol.* 6:120–130.

Hitt, A.L., T.H. Lu, and E.J. Luna. 1994. Ponticulin is an atypical membrane protein. *J. Cell Biol.* 126:1421–1431.

Hock, R.S., and J.S. Condeelis. 1987. Isolation of 240-kilodalton actin-binding protein from *Dictyostelium discoideum*. *J. Biol. Chem*. 262:394–400.

Hoffman, E.P., R.H. Brown, and L.M. Kunkel. 1987. Dystrophin, the protein product of the Duchenne muscular dystrophy locus. *Cell.* 51:919–928.

Hohmann, H.-P., G. Gerisch, R.W.H. Lee, and W.B. Huttner. 1985. Cell-free sulfation of the contact site A glycoprotein of *Dictyostelium discoideum* and of a partially glycosylated precursor. *J. Biol. Chem.* 260:13869–13878.

Ikonen, E., B. de Almeid, K.R. Fath, D.R. Burgess, K. Ashman, K. Simons, and J. Stow. 1997. Myosin II is associated with Golgi membranes: identification of p200 as nonmuscle myosin II on Golgi derived vesicles. *J. Cell Sci.* 110: 2155–2164.

Jenne, N., R. Rauchenberger, U. Hacker, T. Kast, and M. Maniak. 1998. Targeted gene disruption reveals a role for vacuolin B in the late endocytic pathway and exocytosis. *J. Cell Sci.* 111:61–70.

Jermyn, K.A., M. Berks, R.R. Kay, and J.E. Williams. 1987. Two distinct classes of prestalk-enriched mRNA sequences in *Dictyostelium discoideum. Development.* 100:745–755.

Jung, E., P. Fucini, M. Stewart, A.A. Noegel, and M. Schleicher. 1996. Linking microfilaments to intracellular membranes: the actin-binding and vesicle-associated protein comitin exhibits a mannose-specific lectin activity. *EMBO (Eur. Mol. Biol. Organ.) J.* 15:1238–1246.

Kimmel, A.R., and R.A. Firtel. 1983. Sequence organization in *Dictyostelium*: unique structure at the 5′-ends of protein coding genes. *Nucleic Acids Res.* 11:541–552.

Kreitmeier, M., G. Gerisch, C. Heizer, and A. Müller-Taubenberger. 1995. A talin homologue of *Dictyostelium* rapidly assembles at the leading edge of cells in response to chemoattractant. *J. Cell Biol.* 129:179–188.

Kuspa, A., D. Maghakian, P. Bergesch, and W.F. Loomis. 1992. Physical mapping of genes to specific chromosomes in *Dictyostelium discoideum*. *Genomics.* 13:49–61.

Kuspa, A., and W.F. Loomis. 1996*a*. Analysis of the *Dictyostelium discoideum* genome. *In* Analysis of non-mammalian genomes—a practical guide. B. Birren, and E. Lai, editors. Academic Press, New York. 293–318.

Kuspa, A., and W.F. Loomis. 1996*b*. Ordered yeast artificial chromosome clones representing the *Dictyostelium discoideum* genome. *Proc. Natl. Acad. Sci. USA*. 93:5562–5566.

Kuznetsov, S.A., G.M. Langford, and D.G. Weiss. 1992. Actin-dependent organelle movement in squid axoplasm. *Nature*. 356:722–725.

Laemmli, U.K. 1970. Cleavage of structural proteins during assembly of the head of bacteriophage T4. *Nature.* 227:680–685.

Liu, C.-G., C. Maercker, M.J. Castañon, R. Hauptman, and G. Wiche. 1996. Human plectin: organization of the gene, sequence analysis, and chromosome localization (8q24). *Proc. Natl. Acad. Sci. USA*. 93:4278–4283.

Liu, G., L. Thomas, R.A. Warren, C.A. Enns, C. Cunningham, J.H. Hartwig, and G. Thomas. 1997. Cytoskeletal protein ABP-280 directs the intracellular trafficking of furin and modulates proprotein processing in the endocytic pathway. *J. Cell Biol.* 139:1719–1733.

Loomis, W.F. 1969. Developmental regulation of alkaline phosphatase in *D. discoideum*. *J. Bacteriol*. 100:417–422.

Loomis, W.F., and A. Kuspa. 1984. Biochemical and genetic analysis of prestalk specific acid phosphatase in *Dictyostelium. Dev. Biol.* 102:498–503.

Lupas, A., M. Van Dyke, and J. Stock. 1991. Predicting coiled coils from protein sequences. *Science.* 252:1162–1164.

Maniak, M., R. Rauchenberger, R. Albrecht, J. Murphy, and G. Gerisch. 1995. Coronin involved in phagocytosis. Dynamics of particle-induced relocalization visualized by a green fluorescent protein tag. *Cell*. 83:915–924.

Mann, S.K.O., P.N. Devreotes, S. Eliott, K. Jermyn, A. Kuspa, M. Fechheimer, R. Furukawa, C.A. Parent, J. Segall, G. Shaulsky, et al. 1994. Cell biological, molecular genetic, and biochemical methods to examine *Dictyostelium*. *In* Cell Biology: A Laboratory Handbook. Vol. 1. J.E. Celis, editor. Academic Press, San Diego, CA. 412–451.

Matsudaira, P. 1991. Modular organization of actin crosslinking proteins. *Trends Biochem. Sci.* 16:87–92.

Mermall, V., P.L. Post, and M.S. Mooseker. 1998. Unconventional myosins in cell movement, membrane traffic and signal transduction. *Science*. 279:527–533.

Monnat, J., U. Hacker, H. Geissler, R. Rauchenberger, E.M. Neuhaus, M. Maniak, and T. Soldati. 1997. *Dictyostelium discoideum* protein disulfide isomerase, an endoplasmic reticulum resident enzyme lacking a KDEL-type retrieval signal. *FEBS Lett.* 418:357–362.

Müsch, A., D. Cohen, and E. Rodriguez-Boulan. 1997. Myosin II is involved in the production of constitutive transport vesicles from the TGN. *J. Cell Biol.* 138:291–306.

Neujahr, R., R. Albrecht, J. Köhler, M. Matzner, J.-M. Schwartz, M. Westphal, and G. Gerisch. 1998. Microtubule mediated centrosome motility and the positioning of cleavage furrows in multinucleate myosin II null cells. *J. Cell Sci.* 111:1227–1240.

Newell, P.C., A. Telser, and M. Sussmann. 1969. Alternative developmental pathways determined by environmental conditions in the cellular slime mold *Dictyostelium discoideum*. *J. Bacteriol.* 100:763–768.

Noegel, A.A., B.A. Metz, and K.L. Williams. 1985. Developmentally regulated transcription of *Dictyostelium discoideum* plasmid Ddp1. *EMBO (Eur. Mol. Biol. Organ.) J.* 4:3797–3803.

Noegel, A.A., G. Gerisch, J. Stadler, and M. Westphal. 1986. Complete sequence and transcript regulation of a cell adhesion protein from aggregating *Dictyostelium* cells. *EMBO (Eur. Mol. Biol. Organ.) J.* 5:1473–1476.

Noegel, A.A., W. Witke, and M. Schleicher. 1987. Calcium-sensitive non-muscle α-actinin contains EF-hand structures and highly conserved regions. *FEBS Lett.* 221:391–396.

Noegel, A.A., S. Rapp, F. Lottspeich, M. Schleicher, and M. Stewart. 1989. The *Dictyostelium* gelation factor shares a putative actin-binding site with α-actinin and dystrophin and also has a rod domain containing six 100 residue motifs that appear to have a cross-β conformation. *J. Cell Biol.* 108:607–618.

Noegel, A.A., and E. Luna. 1995. The *Dictyostelium* cytoskeleton. *Experientia.* 51:1135–1143.

Noegel, A.A., F. Rivero, P. Fucini, E. Bracco, K.P. Janssen, and M. Schleicher. 1997. Actin binding proteins: role and regulation. *In Dictyostelium*, A Model System for Cell and Developmental Biology. Y. Maeda, K. Inouye, and I. Takeuchi, editors. Universal Academy Press, Inc., Tokyo. 33–42.

Pears, C.J., and J.G. Williams. 1987. Identification of a DNA sequence element required for the efficient expression of a developmentally regulated and cAMP-inducible gene of *Dictyostelium discoideum. EMBO (Eur. Mol. Biol. Organ.) J.* 6:195–200.

Poole, S.J., and R.A. Firtel. 1984. Conserved structural features are found upstream from the three coordinately regulated discoidin I genes of *Dictyostelium discoideum*. *J. Mol. Biol.* 172:203–220.

Prassler, J., S. Stocker, G. Marriot, M. Heidecker, J. Kellermann, and G. Gerisch. 1997. Interaction of a *Dictyostelium* member of the plastin/fimbrin family with actin filaments and actin-myosin complexes. *Mol. Biol. Cell.* 8:83–95.

Rivero, F., B. Köppel, B. Peracino, S. Bozzaro, F. Siegert, C.J. Weijer, M. Schleicher, R. Albrecht, and A.A. Noegel. 1996*a*. The role of the cortical cytoskeleton: F-actin crosslinking proteins protect against osmotic shock

stress, ensure cell size, cell shape and motility and contribute to phagocytosis and development. *J. Cell Sci.* 109:2679–2691.

Rivero, F., R. Furukawa, A.A. Noegel, and M. Fechheimer. 1996*b*. *Dictyostelium discoideum* cells lacking the 34,000-dalton actin-binding protein can grow, locomote and develop, but exhibit defects in regulation of cell structure and movement: a case of partial redundancy. *J. Cell Biol.* 135:965–980.

Sambrook, J., E.F. Fritsch, and T. Maniatis. 1989. Molecular Cloning. A Laboratory Manual. 2nd edition. Cold Spring Harbor Laboratory Press, Cold Spring Harbor, NY.

Scheel, J., K. Ziegelbauer, T. Kupke, B.M. Humbel, A.A. Noegel, G. Gerisch, and M. Schleicher. 1989. Hisactophilin, a histidine-rich actin-binding protein from *Dictyostelium* amoebae. *J. Biol. Chem.* 264:2832–2839.

Schleicher, M., G. Gerisch, and G. Isenberg. 1984. New actin-binding proteins from *Dictyostelium discoideum*. *EMBO (Eur. Mol. Biol. Organ.) J.* 3:2095–2100.

Schleicher, M., A. Noegel, T. Schwarz, E. Wallraff, M. Brink, J. Faix, G. Gerisch, and G. Isenberg. 1988. A *Dictyostelium* mutant with severe defects in alpha-actinin: its characterization using cDNA probes and monoclonal antibodies. *J. Cell Sci.* 90:59–71.

Simpson, P.A., J.A. Spudich, and P. Parham. 1984. Monoclonal antibodies prepared against *Dictyostelium* actin: characterization and interaction with actin. *J. Cell Biol.* 99:287–295.

Sternfeld, J., and C.N. David. 1981. Cell sorting during pattern formation in *Dictyostelium. Differentiation.* 20:10–21.

Tabor, S., and C.C. Richardson. 1992. A bacteriophage T7 RNA polymerase/promoter system for controlled exclusive expression of specific genes. *Biotechnology*. 24:280–284.

Takeuchi, I., T. Kakutani, and M. Tasaka. 1988. Cell behavior during formation of prestalk/prespore pattern in submerged agglomerates of *Dictyostelium discoideum. Dev. Genet.* 9:607–614.

Titus, M., A. Kuspa, and W.F. Loomis. 1994. The myosin family of *Dictyostelium*: a YAC-based approach to identifying members of a gene family. *Proc. Natl. Acad. Sci. USA*. 91:9446–9450.

Towbin, H., T. Staehelin, and J. Gordon. 1979. Electrophoretic transfer of proteins from polyacrylamide gels to nitrocellulose sheets: procedure and some applications. *Proc. Natl. Acad. Sci. USA*.76:4350–4354.

Troll, H., D. Malchow, A. Müller-Taubenberger, B. Humbl, F. Lottspeich, M. Ecke, G. Gerisch, A. Schmid, and R. Benz. 1992. Purification, functional characterization, and cDNA sequencing of mitochondrial porin from *Dictyostelium discoideum*. *J. Biol. Chem*. 267:21072–21079.

Uyeda, T.Q.P., and M.A. Titus. 1997. The myosins of *Dictyostelium*. *In Dictyostelium*, a model system for cell and developmental biology. Y. Maeda, K. Inouye, and I. Takeuchi, editors. Universal Academy Press, Inc., Tokyo. 43–64.

Verkerke-van Wijk, I., and P. Schaap. 1997. cAMP, a signal for survival. *In Dictyostelium*, A Model System for Cell and Developmental Biology. Y. Maeda, K. Inouye, and I. Takeuchi, editors. Universal Academy Press, Inc., Tokyo. 145–162.

Weiner, O.H., J. Murphy, G. Griffiths, M. Schleicher, and A.A. Noegel. 1993. The actin-binding protein comitin (p24) is a component of the Golgi apparatus. *J. Cell Biol.* 123:23–34.

Wessels, D., and D.R. Soll. 1990. Myosin II heavy chain null mutants exhibit defective intracellular particle movement. *J. Cell Biol*. 111:1137–1148.

Westphal, M., A. Jungbluth, M. Heidecker, B. Mühlbauer, C. Heizer, J.-M. Schwarz, G. Marriot, and G. Gerisch. 1997. Microfilament dynamics during cell movement and chemotaxis monitored using a GFP-actin fusion. *Curr. Biol.* 7:176–183.

Williams, J. 1997. Prestalk and stalk cell heterogeneity in *Dictyostelium*. *In Dictyostelium*, a model system for cell and developmental biology. Y. Maeda, K. Inouye, and I. Takeuchi, editors. Universal Academy Press, Inc., Tokyo. 293–304.

Williams, K.L., and P.C. Newell. 1976. A genetic study in the cellular slime mold *Dictyostelium discoideum* using complementation analysis. *Genetics.* 82:287–307.

Witke, W., M. Schleicher, and A.A. Noegel. 1992. Redundancy in the microfilament system: abnormal development of *Dictyostelium* cells lacking two F-actin crosslinking proteins. *Cell.* 68:53–62.

Wong, E.F.S., S.K. Brar, H. Sesaki, C. Yang, and C.-H. Siu. 1996. Molecular cloning and characterization of DdCAD-1, a Ca^{2+}-dependent cell-cell adhesion molecule, in *Dictyostelium discoideum*. *J. Biol. Chem.* 271:16399–16408.

Yan, Y., E. Winograd, A. Viel, T. Cronin, S.C. Harrison, and D. Branton. 1993. Crystal structure of the repetitive segments of spectrin. *Science*. 262:2027–2030.